SCOG JOURNAL

SCIENTIFIC CONTRIBUTION OIL AND GAS

ISSN : 2089-3361

e-ISSN : 2541-0520

VOLUME 47 NO. 1, APRIL 2024

ACCREDITED RISTEK DIKTI
79/E/KPT/2023

Scientific Contributions Oil & Gas, Vol. 47. No. 2, August: 143-158

SCIENTIFIC CONTRIBUTIONS OIL AND GAS
Testing Center for Oil and Gas
LEMIGAS

Journal Homepage:http://www.journal.lemigas.esdm.go.id
ISSN: 2089-3361, e-ISSN: 2541-0520

The Influence of Side-Slip Velocity on Subsurface Displacement

Imam Setiaji Ronoatmojo, Muhammad Burhannudinnur, Yarra Sutadiwiria and Dewi Syavitri

Universitas Trisakti
Kyai Tapa 1 Street, Jakarta, Indonesia

Corresponding author: aji.rono@trisakti.ac.id

Manuscript received: June 26st, 2024; Revised: July 26st, 2024
Approved: July 29st, 2024; Available online: July 31st, 2024

ABSTRACT - This research aimed to determine the influence of side-slip velocity on subsurface displacement during seismic data acquisition. Anisotropy constants were used to determine the depth migration process before stack, which showed inadequate results after data validation. Therefore, the forward modeling of a medium, which comprised anisotropy constants of normal and offset raytracing was conducted to address this problem. The configuration of source to receiver were orthogonal and slant. The results showed that the migration process failed to resolve the geological structures of the position shifting. The configuration of source to receiver were orthogonal and slant. The results show the better continuity of slant and the influence of complex geological structures controls the position shifting, which could not be resolved by the migration process. It could be seen from the random distribution of the normal shift of group velocity and phase velocity, as well as the CDP – CRP shift. It produced wave azimuth rotation in a discontinuity plane, such as fault and anticline ridge. This azimuth rotation was strongly suspected to cause inaccurate anisotropy constants implementation in pre-stack depth migration process.

Keywords: side-slip velocity, anisotropy constants, migration, normal displacement, CDP-CRP displacement.

How to cite this article:

Imam Setiaji Ronoatmojo, Muhammad Burhannudinnur, Yarra Sutadiwiria and Dewi Syavitri, 2024, The Influence of Side-Slip Velocity on Subsurface Displacement, Scientific Contributions Oil and Gas, 47 (2) pp. 143-158. DOI.org/10.29017/SCOG.47.2.1620.

INTRODUCTION

Seismic anisotropy is associated with velocity variations in pre-stack depth migration. This led to the issue of deviated result in time to depth domain transformation, specifically observed when validated with well data. The current research investigated the effect of anisotropic medium on wave velocity, despite the varying constants. Anisotropic medium was designed by using the constants to determine the actual response. Additionally, this was modeled in respect to the previous seismic data interpretation, conducted in Naintupo, Tabul, and Tarakan Formations, found at approximately 1,000 to 3,000 meters beneath the earth surface. The thick intercalation of sand-shale lithology produced anisotropic tendencies, due to the presence of bedding planes. Anisotropic occurrence in sedimentary rocks is related to the sedimentation process of different layers, strata or minerals with various grain sizes. These secondary structures or macro-scale features of rocks were also defined as discontinuities. The influence of anisotropic medium properties was reflected as the difference between group and phase velocities (Ronoatmojo and Burhannudinnur, 2018).

Anisotropy of materials such as the earth must be taken into account during data acquisition and interpretation. According to Sheriff (2002) seismic

anisotropy is defined as seismic velocity variation depending on the propagating direction of either P- or S- waves or polarization (for S-waves). Velocity as a physical parameter plays an important role in seismic exploration, as well as defines anisotropic properties. The estimation accuracy is important, because velocity is a critical parameter that influences the quality of near-surface distortion correction (Taner et.al, 1974), multi-fold data processing (Mayne, 1962) and seismic data migration (Berkhout, 1984; Claerbout, 1985). Physical properties also has an impact on the interval velocity estimation, including the transformation of time to depth using Dix formula and tomographic methods. Therefore, adequate knowledge of lithology and stratigraphy is needed, to observe seismic wave propagating through any anisotropic medium (Domenico, 1984).

Material heterogeneity depends on the difference in physical properties at various positions, particularly when anisotropic nature of matter is manifested as varying wave velocity orientations in various directions. Therefore, the medium is isotropic and homogeneous, contradicting the fact that it is anisotropic and heterogeneous. This depends on the primary arrangement of the rock-forming minerals referred to as microscopic packing (Ullemeyer et al, 2006). Anisotropic tendencies in seismic exploration were observed as the differences in velocity values in the vertical and horizontal directions. These differences tend to appear, specifically when far offsets are used.

In 1932, McCollum and Snell conducted research and reported that the horizontal P-wave velocity of the Lorraine shale in Canada was 1.4 times the vertical P-wave velocity (Levin, 1978). Similarly, various research on anisotropy conducted since the 1950s stated that the tendencies occurred when the thickness of the layer was less than the seismic wavelength propagated in the medium (Postma, 1955; Dellinger, 1991). Meanwhile, evidence of intrinsic anisotropy was obtained from the laboratory analyses of several rock samples related to the change in pressure beneath the surface (Nur, 1969; Dellinger, 1991). Bachman (1979), found transverse isotropy in cores originating from deep sea drilling. Jones and Wang (1981), made similar observations in cores from the Williston Basin, North Dakota.

The application of anisotropic properties was ignored until the 1980s, because most seismic data were recorded in respect to near to medium offsets, even though the medium was not isotropic. It was observed that the use of far offset data, specifically for anisotropic media during NMO or normal move-out process, led to difficulties in obtaining the accurate velocity correction. Another influence of anisotropic properties was observed during migration, where far offset travel time with an angle greater than 40^0 led to energy shifting from the original path to another position, as shown in Figure 1. This refers to the tangent point position of wavefront (Dellinger, 1991).

Anisotropic assumptions such as AVO, or amplitude versus offset analysis, must be taken into account, during seismic data interpretation. Meanwhile, Blangy (1994), and Ruger (1998), made certain corrections to the Aki-Richard equation by inserting anisotropic parameters. The constant estimation could be determined either directly or indirectly. Direct and indirect observations were carried out using VSP data, and reflection or diffraction function, respectively (Ronoatmojo et al, 2010). Diffraction is henomenon of energy scattering at discontinuity plane, so that transmission waves from sources below surface, can be used to determine anisotropic constants. This is done if there are no wells penetrating the area.

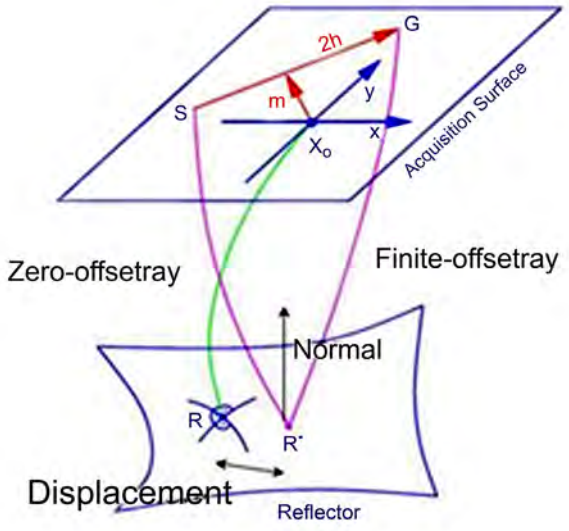

Figure 1
CDP – CRP displacement.

The phase velocity denoted as simply means that the distance traveled per unit time is in the constant phase position, such as in the trough or peak of wave (Sheriff and Geldart, 1995). The process is not similar to the group velocity, which is velocity with energy

propagates from one point to another. For example, in Figure 2, the group velocity $= \frac{\Delta x}{\Delta t_g}$

in waves series. It is described as velocity obtained from the slope of the pulse envelopes top (ABC and AB'C curves). The phase velocity was described as velocity obtained from the slope of a line representing similar phase state, equivalent to $\frac{\Delta x}{\Delta t_p}$. When a pulse is decomposed into frequency components in a Fourier spectrum, the phase and group velocities tend to be similar for all frequency values. Variations in phase velocity relative to the frequency, changes the pulse shape, and the group velocity. The relationship between group and phase velocities in the dispersive medium is expressed in Equation (1):

$$V(\emptyset) = V(\theta) - \lambda \frac{dV(\theta)}{d\lambda} = V(\theta) + \omega \frac{dV(\theta)}{d\omega} \quad (1)$$

where $\frac{dV(\theta)}{d\lambda}$ and $\frac{dV(\theta)}{d\omega}$ are the phase velocity change in varying wavelengths or frequencies. Assuming the phase velocity decreases as the frequency increases, the value obtained would be greater than the group velocity as shown in Figure 2. The phase velocity is less than the group velocity, when it increases with increasing frequency. Furthermore, the difference between these velocities in a dispersive medium was showed by the change in pulse shape. This is caused by alterations in phase velocity with respect to frequency variations. The process does not always occur in every medium, and important in differentiating the occurrence of anisotropy.

In anisotropic medium, the relationship between group *V(φ)* and phase velocities *V(*θ*)* is expressed in Equation (2):

$$V(\phi)^2 = \mathrm{V}(\theta)^2 + \left(\frac{d\mathrm{V}(\theta)}{d(\theta)}\right)^2 \quad (2)$$

The difference in Equation 2 was based on variations in phase velocity in respect to wavefront normal, where θ is the phase angle and ϕ the group angle. However, the difference between the group and phase velocities in anisotropic medium determines the magnitude of the position shifting beneath the surface. The larger the difference, the greater the shifting, or the more anisotropic the medium, the further the position of a point would be shifted from the origin.

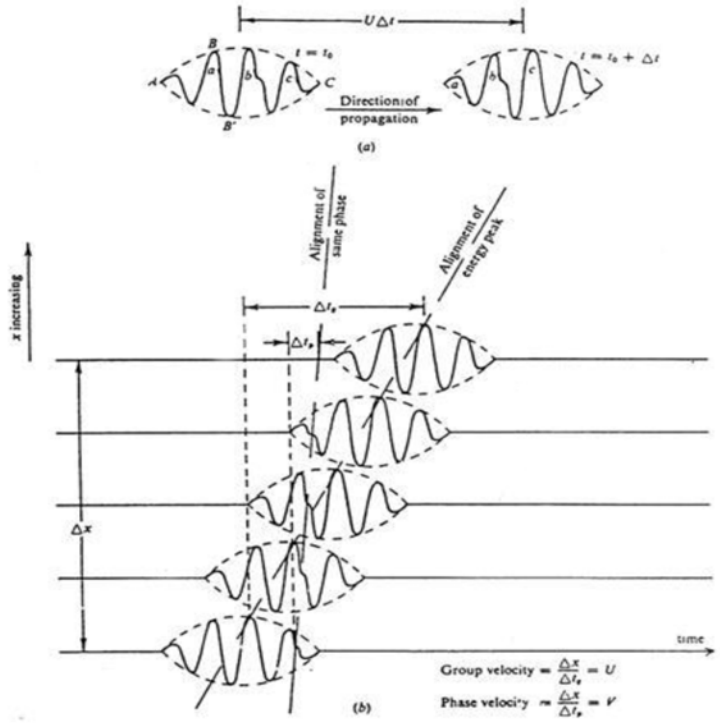

Figure 2
Group and phase velocities in a dispersive medium (Sheriff and Geldart, 1995).

Preliminary investigation on the relationship between group and phase velocities, alongside technological advances regarding the use of data with large offsets and multi azimuth, led to the problem of velocity anisotropy. An overview of the geometry between group and phase velocities is needed to understand position displacement. Byun (1984; 2000), conducted research on the elliptic nature of the raypath velocity associated with the group velocity. Generally, assuming a medium is anisotropic, velocity in the direction of wave propagation or seismic energy would differ from the one in the perpendicular wavefront The geometry described by Byun (1984) in Figure 3, shows that α is the angle formed by the group trajectory with the normal of the boundary plane, and γ is the angle between the axis and the normal of the boundary plane.

Wave surface is the points present in response to the source. Meanwhile, for anisotropic medium, this elliptical figure is determined using the ellipse equation:

$$\mathrm{V}(\phi)^{-2} = {v_{az}}^{-2}cos^2\phi + {v_{ax}}^{-2}sin^2\phi \quad (3)$$

where and are the phase velocities along the z and x symmetry axes of the ellipse, while is the group (raypath) velocity at angle from the axis. Geometrically, the relationship and V(θ) could be defined using Equation (4):

$$V(\theta) = V(\phi)\cos(\phi - \theta) \quad (4)$$

assuming,

$$\tan\theta = \left(\frac{v_{az}}{v_{ax}}\right)^2 tan\phi \quad (5)$$

the relationship between V(θ) with and could be expressed as:

$$\mathrm{V}(\theta)^2 = {v_{az}}^2cos^2\theta + {v_{ax}}^2sin^2\theta \quad (6)$$

The relationship between group and phase velocities in Figure 4, shows that if the normal of phase angle is squeezed with group angle, then the right-angled triangle SGF and SGF' would appear. Furthermore, phase and group velocity changes were detected in SGF and SGF' right-angled triangles, respectively. So by placing the group angle and phase angle on the same normal line axis, the geometric solution can be done more clearly. It can be seen that the group angle is always greater than the phase angle. It is understandable that the elliptical tendency results in decrease of the phase angle. So the stronger the anisotropy, the more phase angle shifts to the normal axis.

Considering SGF:

$$cos(\phi - \theta) = \frac{V(\theta)}{V(\phi)} \quad (7)$$

So,

$$cos(\phi - \theta) = \frac{V(\phi)}{\sqrt{V(\phi)^2 + \left(\frac{dV(\phi)}{d\phi}\right)^2}} \quad (8)$$

Regarding Equations (7) and (8), in anisotropic medium, the group velocity is greater than the phase velocity. It is the sum of the phase (perpendicular to wavefront) and side-slip velocity. Therefore, the greater the side-slip velocity , the more the position of subsurface point would be shifted, including increasing the elliptic factor of the group velocity. Assuming the equation used to determine the relationship between phase velocity and anisotropy parameter is substituted into Equation 9, it would produce a solution for measuring anisotropy parameter indirectly.

$$V(\theta) = \frac{V(\phi)^2}{\sqrt{V(\phi)^2 + \left(\frac{dV(\phi)}{d\phi}\right)^2}} \quad (9)$$

Thus, the above equation demonstrates goniometrically that the presence of anisotropic tendency will result in position shifting. The following work is to prove with an illumination modeling, which includes an anisotropic model and wave propagation which is considered by this model. It is done to find out the implication of structural complexity.

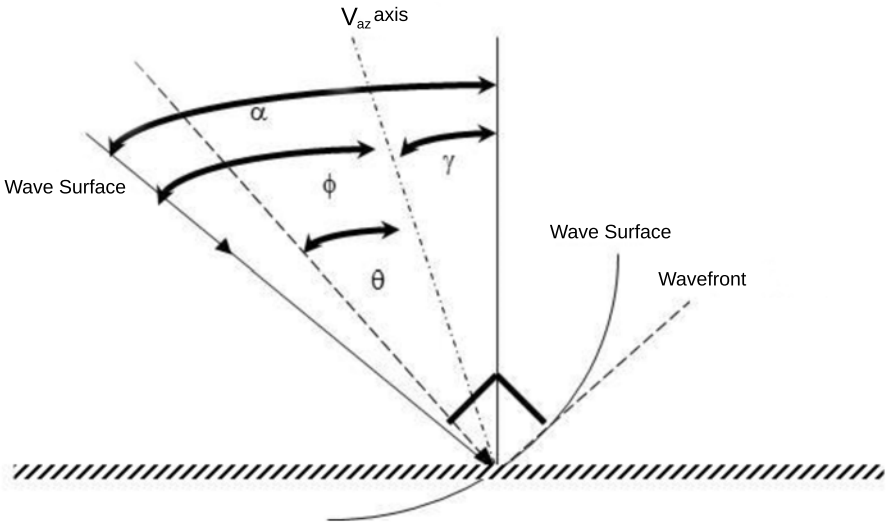

Figure 3
Geometry of raypath and phase in boundary plane (Byun, 1984).

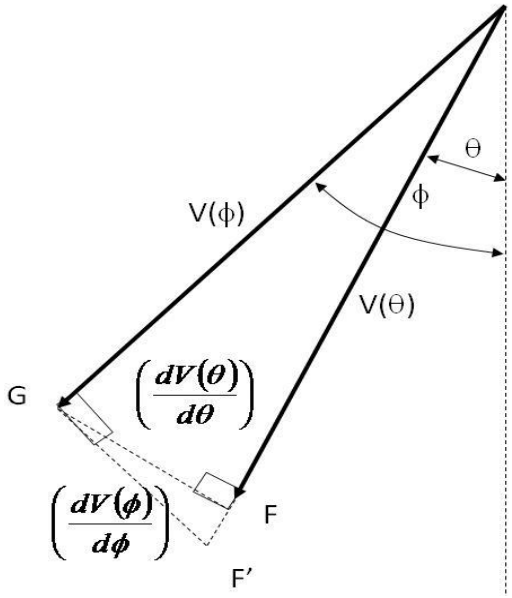

Figure 4
Geometry of group and phase velocities (Byun, 1984).

METHODOLOGY

Anisotropic properties could shift subsurface position as shown in Figure 1. However, during the migration process, this principle is not neglected, but it resulting in inaccurate position of the seismic to the well data. Therefore in this research, it was began from a forward modeling which is generated from three-dimensional seismic data, built from Pre-stack Depth Migration (PSDM). Anisotropic parameters were determined from VSP of three existing markers, whose constants were calculated based on the average velocity of each. This was considered as vertical (), and angle velocity () for the far offset.

Table 1
Anisotropy constants (and)

Marker	δ		ε	
	Well-A	Well-B	Well-A	Well-B
1	0.23	0.4	0.18	0.38
2	0.31	0.52	0.31	0.49
3	0.35	0.63	0.36	0.67

The results of the previously interpreted seismic data were used as model input for carrying out illumination work on wave propagation. This was realized by entering anisotropy constant value as a factor that would correct the group velocity. Theoretically, anisotropic parameter was applied based on the geometry of the material, including velocity function, phase and wavelength. It failed to consider the vertical resolution, due to the large thickness of the inter horizons, which exceeded the existing resolution. However, the lateral resolution was calculated based on the Fresnel zone. After wave travel time was obtained, the position of each subsurface data set (CDP gather) was determined in respect to the depth value. This was also defined through the layer boundary plane, represented by the horizon. Acquisition lay-out was simulated orthogonally and slanted, to compare several items related to fold distribution, offset orientation and azimuth. The complete sequence of the work flow is shown in Figure 5.

The geological structure examined in Figure 6, is a giant W-E fault structure that extends to an W-E anticline ridge. This small fault is perpendicular to the giant W-E structure with N-S orientation. Northward to the anticline ridge, is a homocline with a dip. Meanwhile, a syncline valley is found towards the south. This interesting model, has stratigraphic anisotropy constants, as well as a fairly complex geological structure, which have an impact in the bending of wave propagation.

The two types of layouts were designed orthogonally and slanted, with each receiver lines oriented in N-S direction. Therefore, it was crossed perpendicularly through most of the structures, except for N-S. In Figure 7a, the orthogonal layout, referred to as the source line orientation (W-E) is perpendicular to the receiver line, where SLI (Source Line Interval) and RLI (Receiver Line Interval) are 800 meters and 300 meters, respectively, and the number of active channels is 2.016 units. Meanwhile, the other layout is slanted as shown in Figure 7b with the source line orientation (N-S) forming an oblique angle with the receiver line, where SLI and RLI is 800 meters and 250 meters, respectively, and the number of active channels is 2.000 units.

The slant mode was used to determine, whether the source line designed at an angle to the receiver, influences shifting continuity. CDP is subsurface point, reflected at the layer boundary plane, but due to anisotropic characteristic, it was shifted by the slide slip velocity, and was referred to as CDP – CRP displacement. The difference between orthogonal and slant modes were observed in Figures 8a and b, where the design in the cross section, showed the richer data filling in the slant mode. In this case, the slant mode offsets filling more in the existing vertical grids, and when combined with the cross-line offsets, data continuities would be better. This is important to strengthen the coherency of the data to be sampled. However, there is need for further investigation to ascertain whether data continuity would affect anisotropic problems.

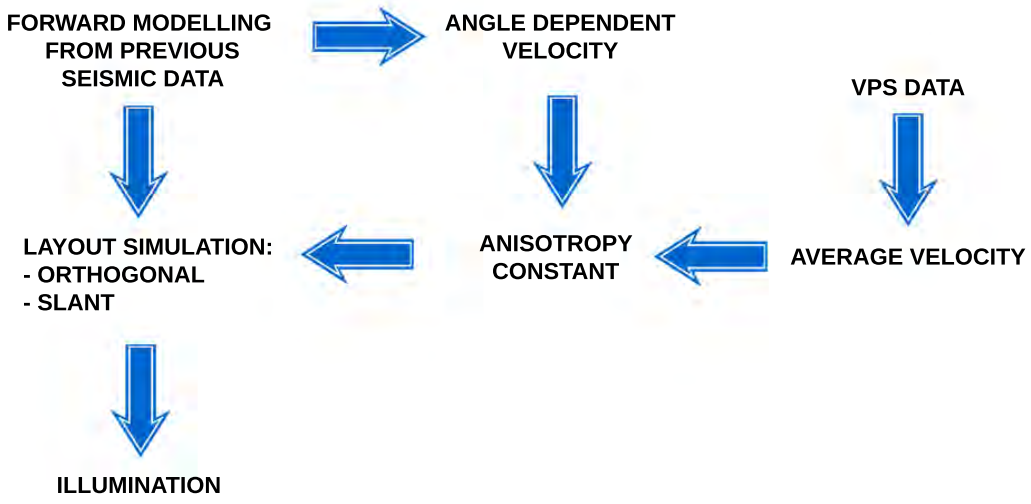

Figure 5
Workflow.

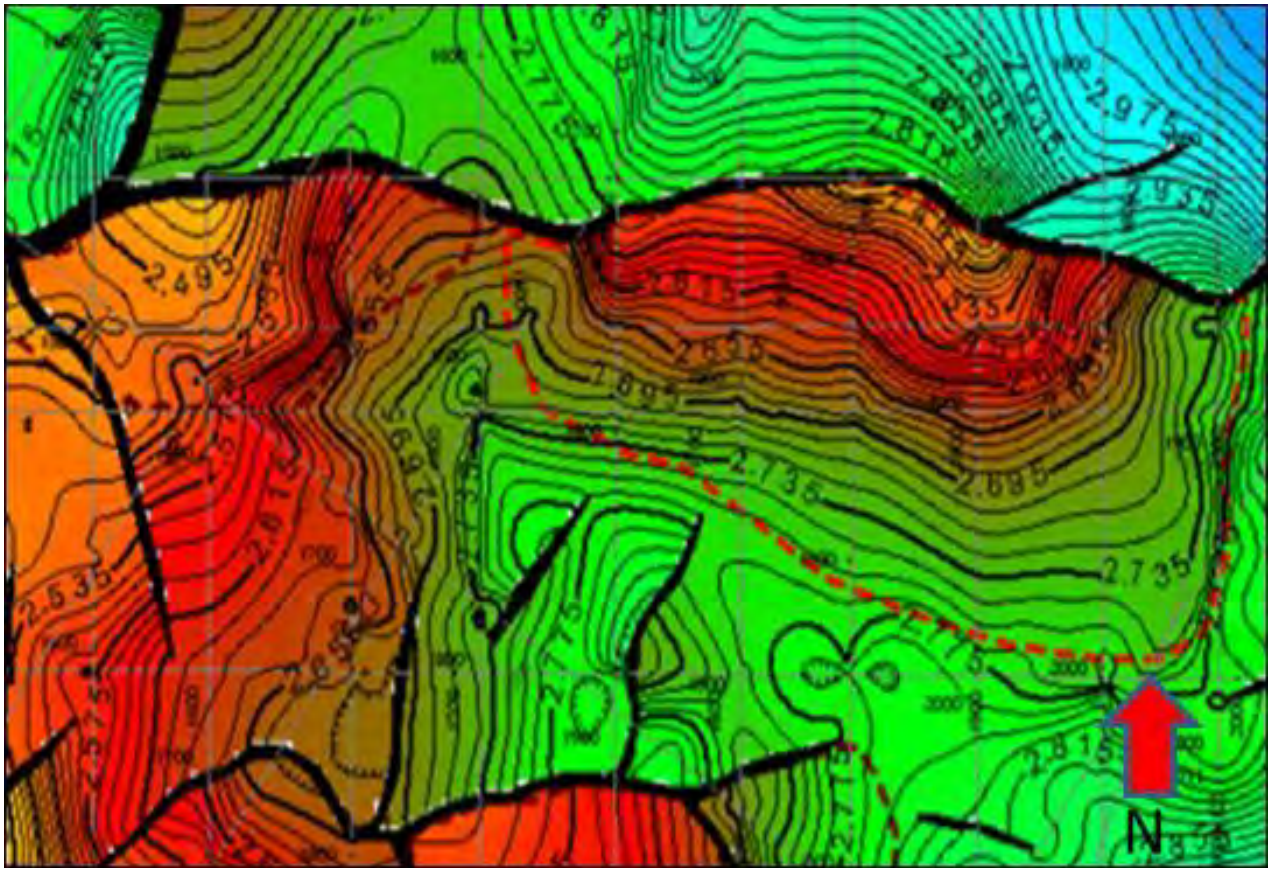

Figure 6
Geological structure of the model to be studied.

(a)

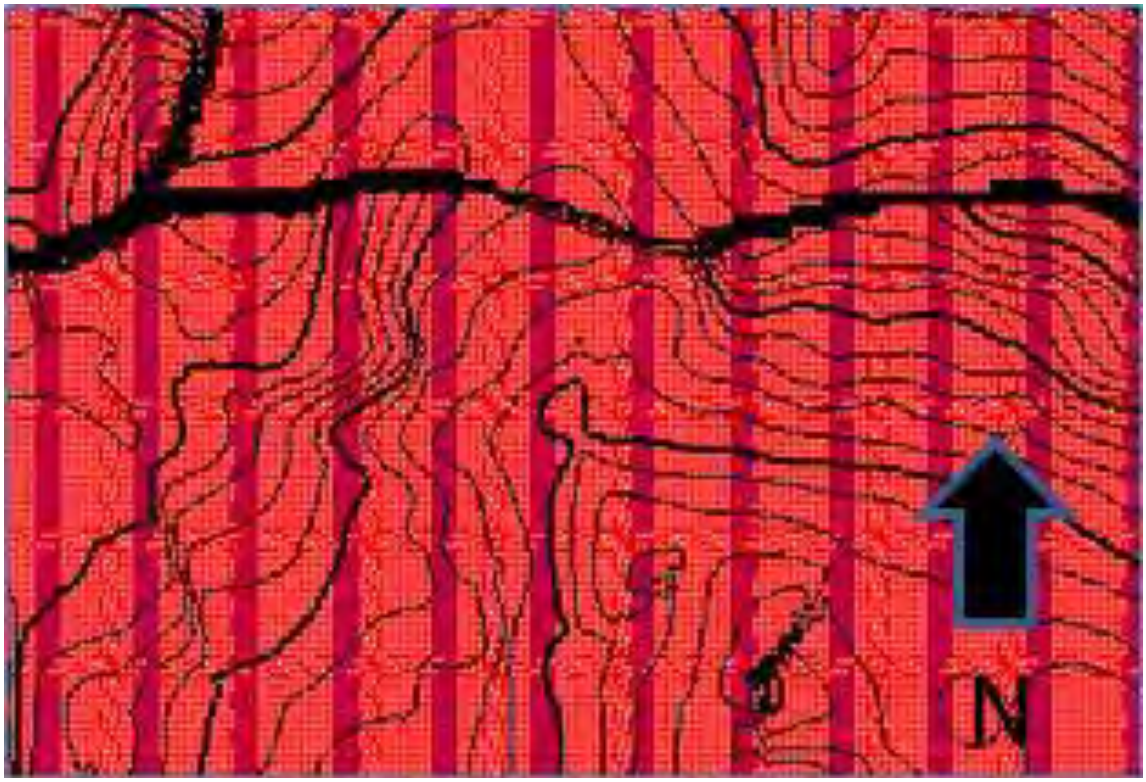

(b)

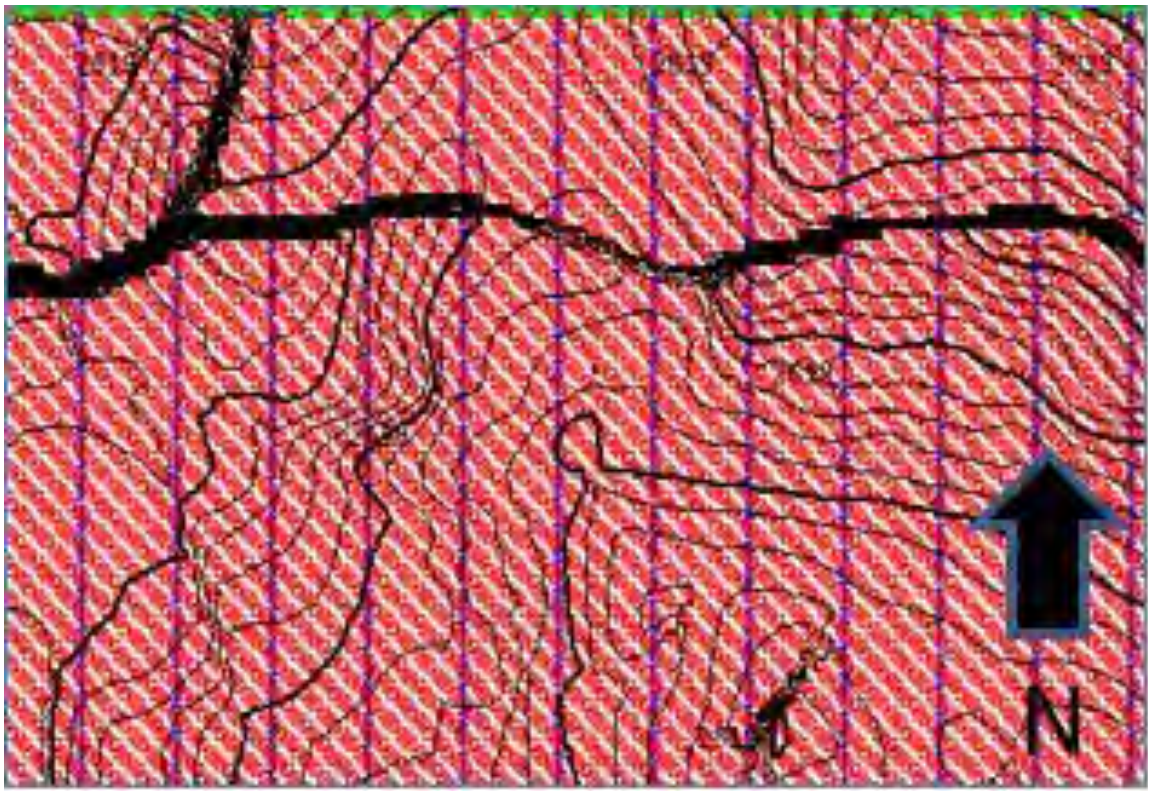

Figure 7
Lay-out: (a) orthogonal, (b) slant which is simulated to describe the ray-path configuration during data acquisition.

(a)

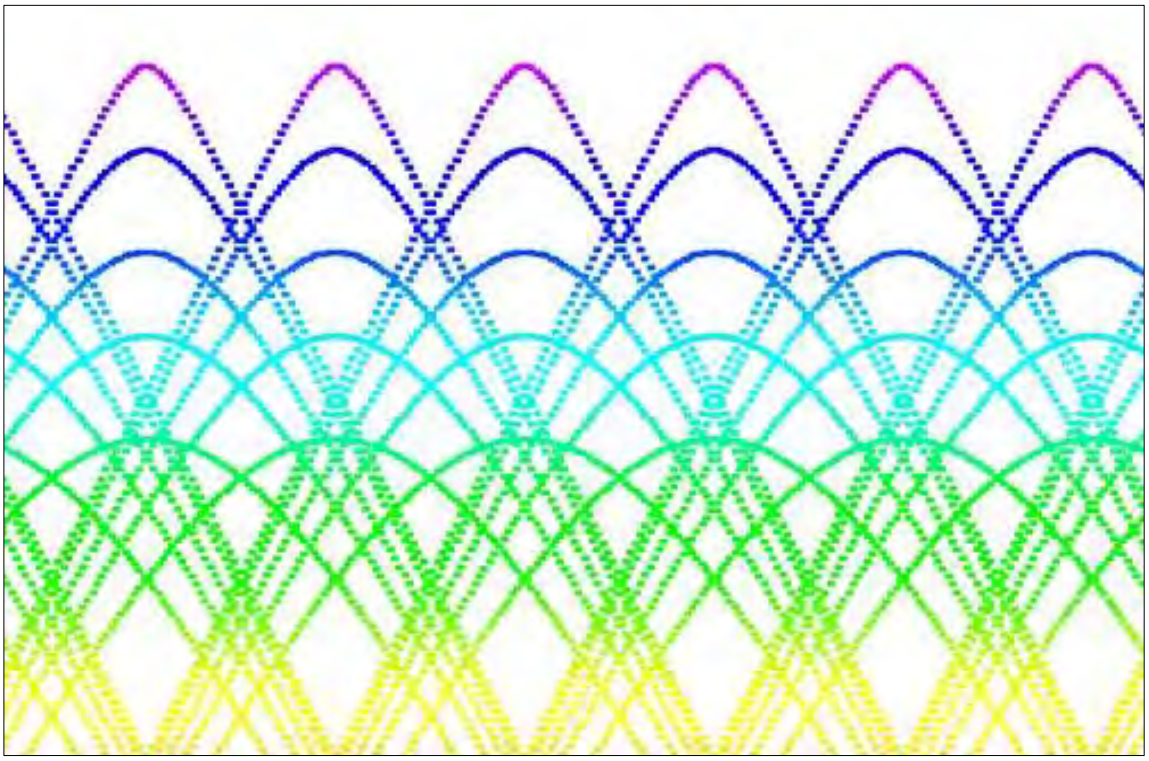

(b)

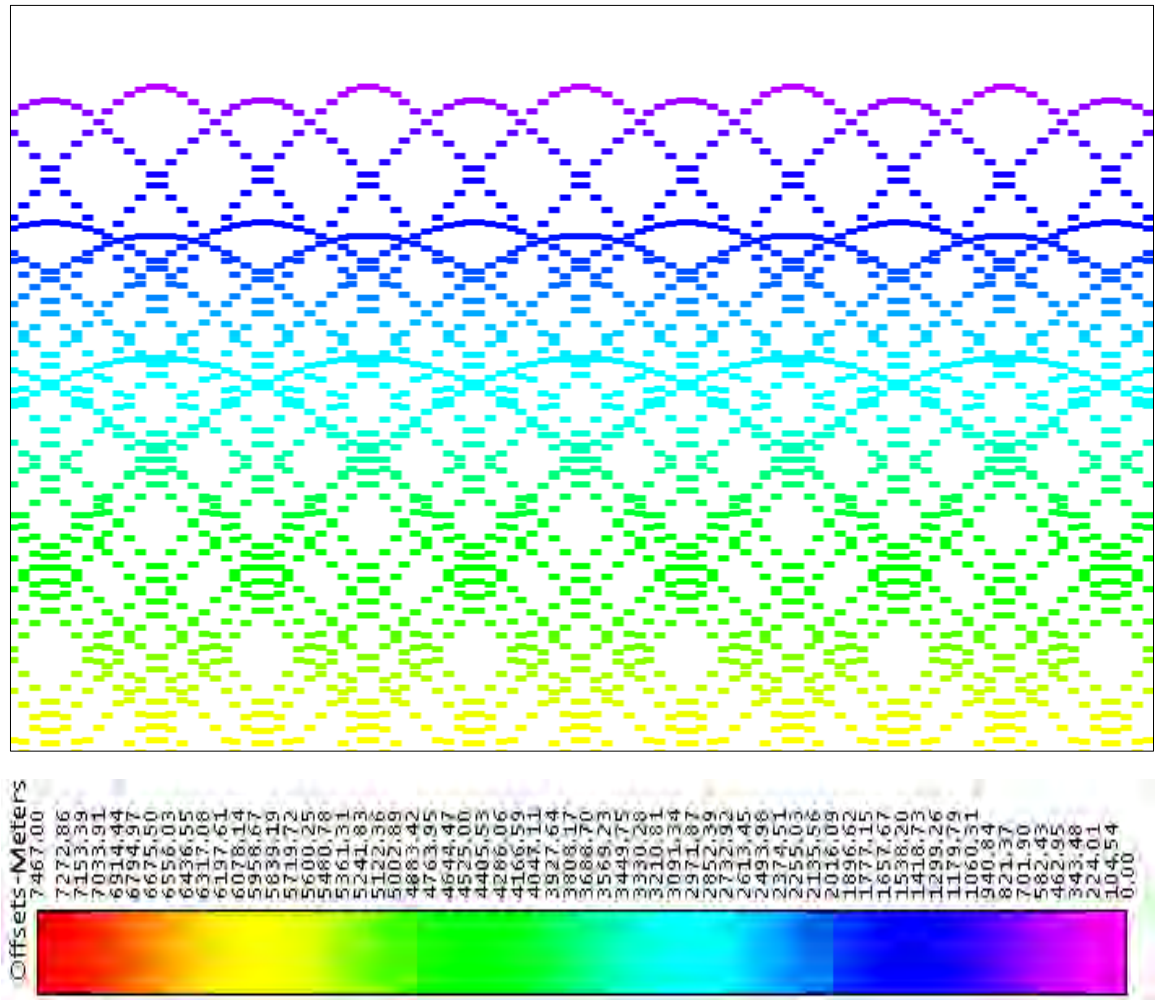

Figure 8
Lay-out in-line section: (a) orthogonal, (b) slant which shows the different configurations of the offset distribution transversely with the color indicating depth where the red color on the color bar scale showing the longest offset.

RESULT AND DISCUSSION

Normal Raytracing

After illumination, the maximum incident angle distribution was obtained from each horizon. Additionally, the group angle was formed with respect to the normal of the bedding boundary plane. The distribution obtained for each horizon showed that the value of the maximum incident angle for the shallowest horizon, was greater than the maximum incident angle for the deeper horizon. Meanwhile, the image of the slant mode was slightly different from the orthogonal. The faults and anticline ridges had a tendency to increase the value of the maximum incident angle as shown in Figure 9.

The normal of a layer boundary plane, is assumed to be the normal of group angle, while the normal of phase angle is a line perpendicular to wavefront. Figure 9 shows that in respect to the shifting between group and phase normal, the highest shift was larger for faults and anticline ridges, while synclines had lower shift. Furthermore, the complex features were observed in the deeper Horizons 2 and 3, caused by the raypath model, which was not bent above Horizon 1.

The shift was also observed in the azimuth direction as shown in Figure 10. When combined with the previous attributes, it was used to explain the vector of normal shifting. Additionally, the influence of the geological structure depended on the azimuth distribution.

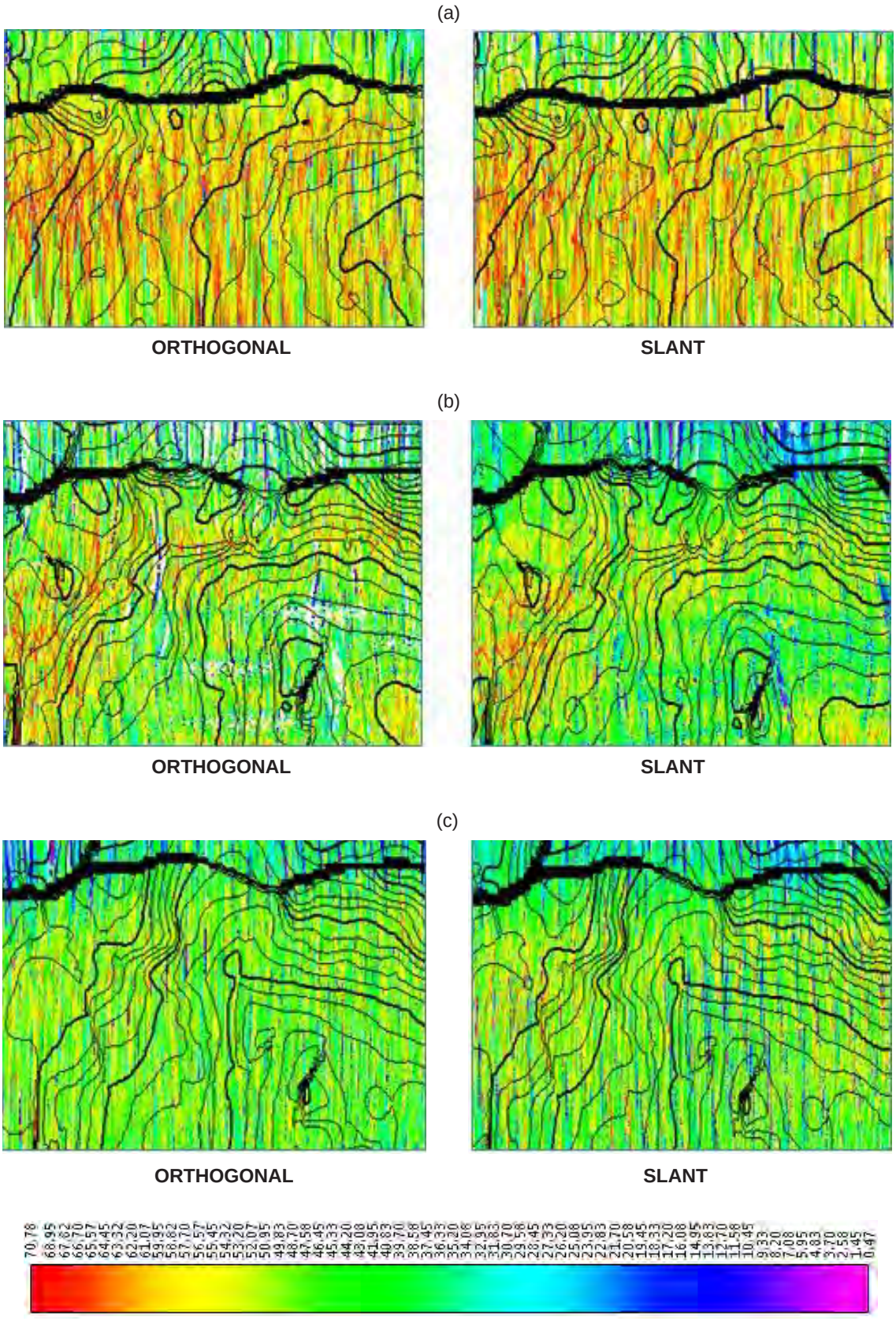

Figure 9
Maximum incident angle: (a) Horizon 1, (b) Horizon 2, (c) Horizon 3; it can be seen that the distribution of maximum incident angles for the shallower horizon is higher.

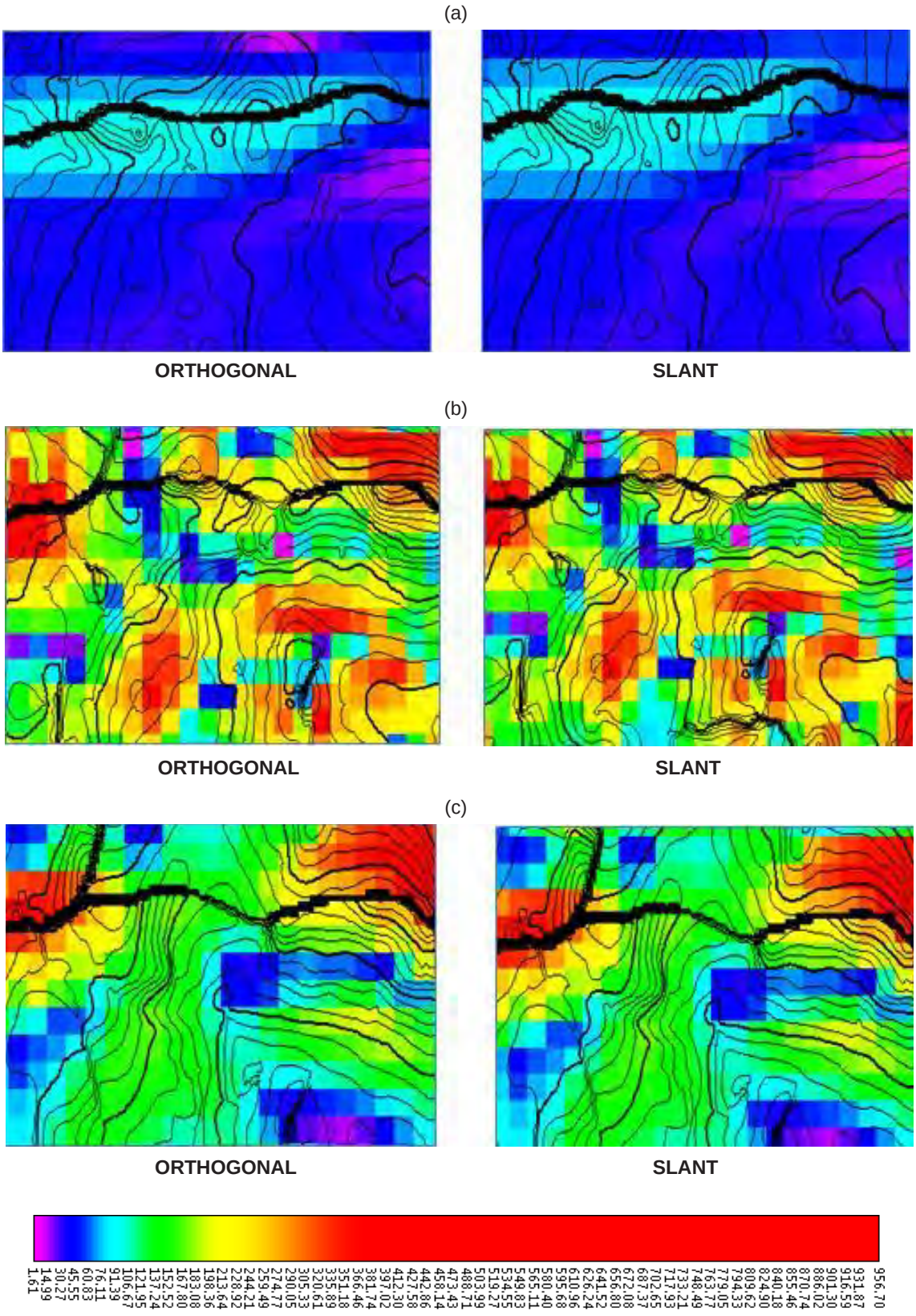

Figure 10
Normal displacement: (a) Horizon 1, (b) Horizon 2, (c) Horizon 3; it can be seen that the distribution of normal displacement for the shallower horizon is lower.

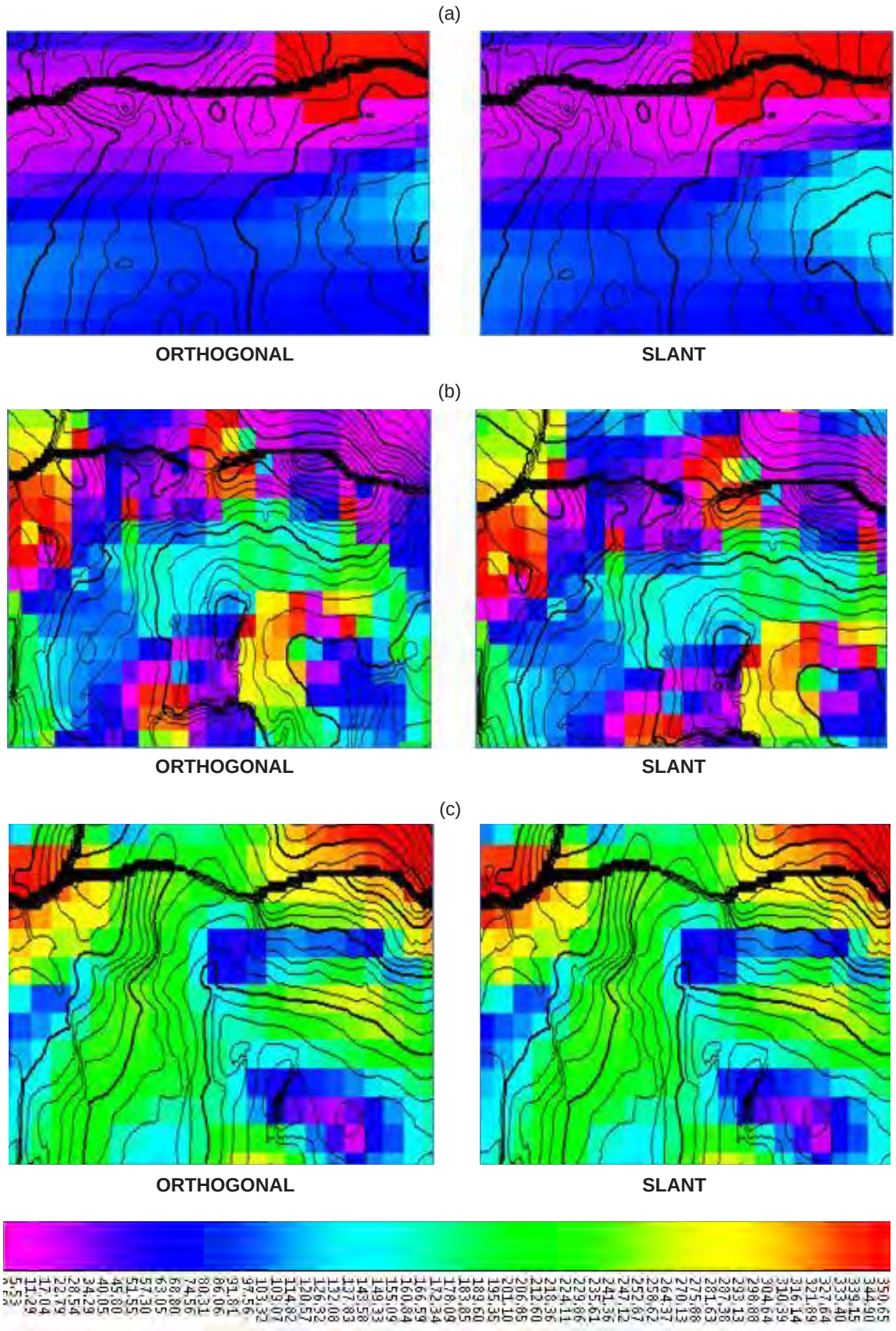

Figure 11
Normal azimuth: (a) Horizon 1, (b) Horizon 2, (c) Horizon 3; it can be seen that the distribution of normal azimuth for the shallower horizon is lower.

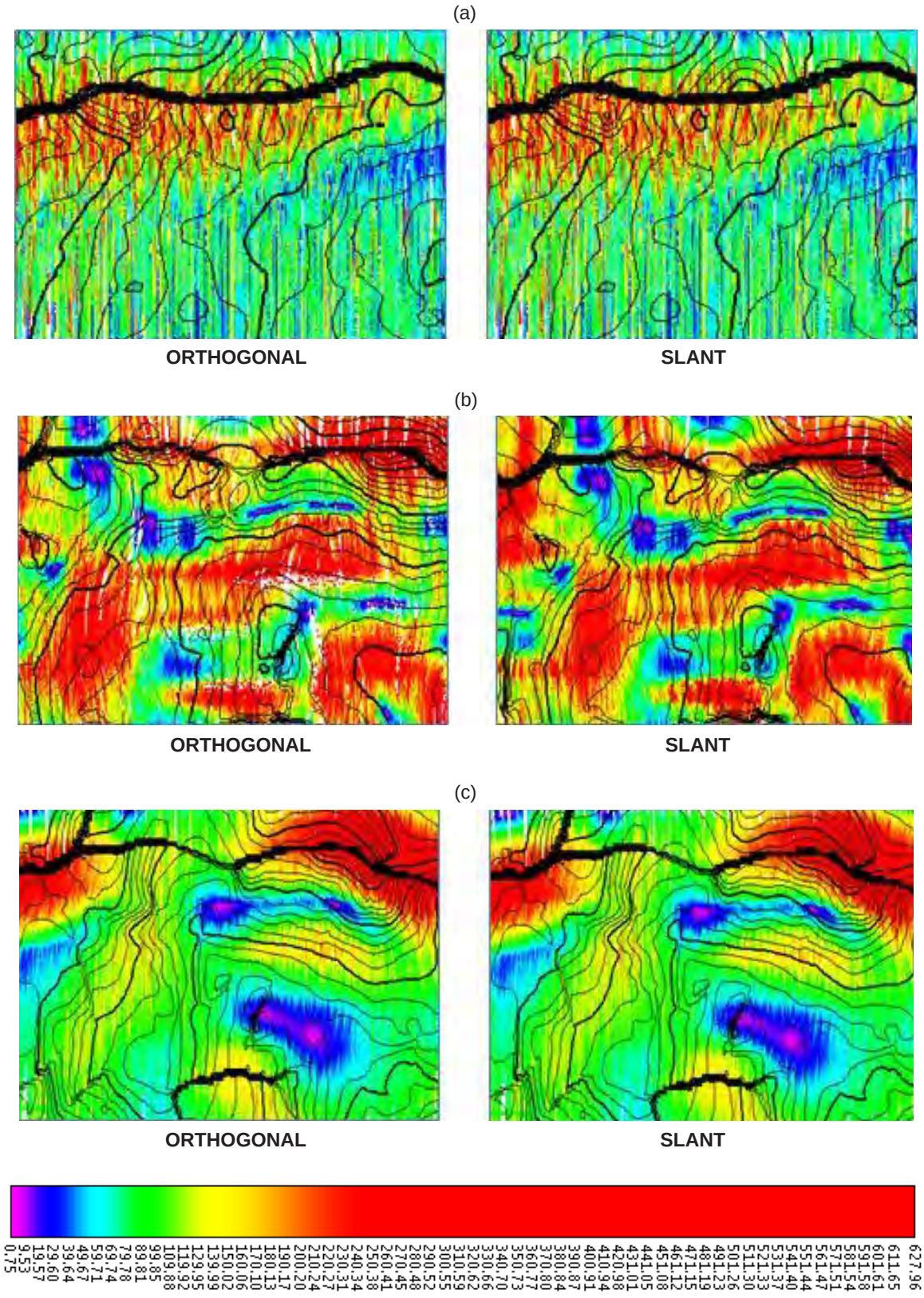

Figure 12
CDP – CRP displacement: (a) Horizon 1, (b) Horizon 2, (c) Horizon 3; it can be seen that the distribution of CDP-CRP displacement for the deeper horizon is more complicated

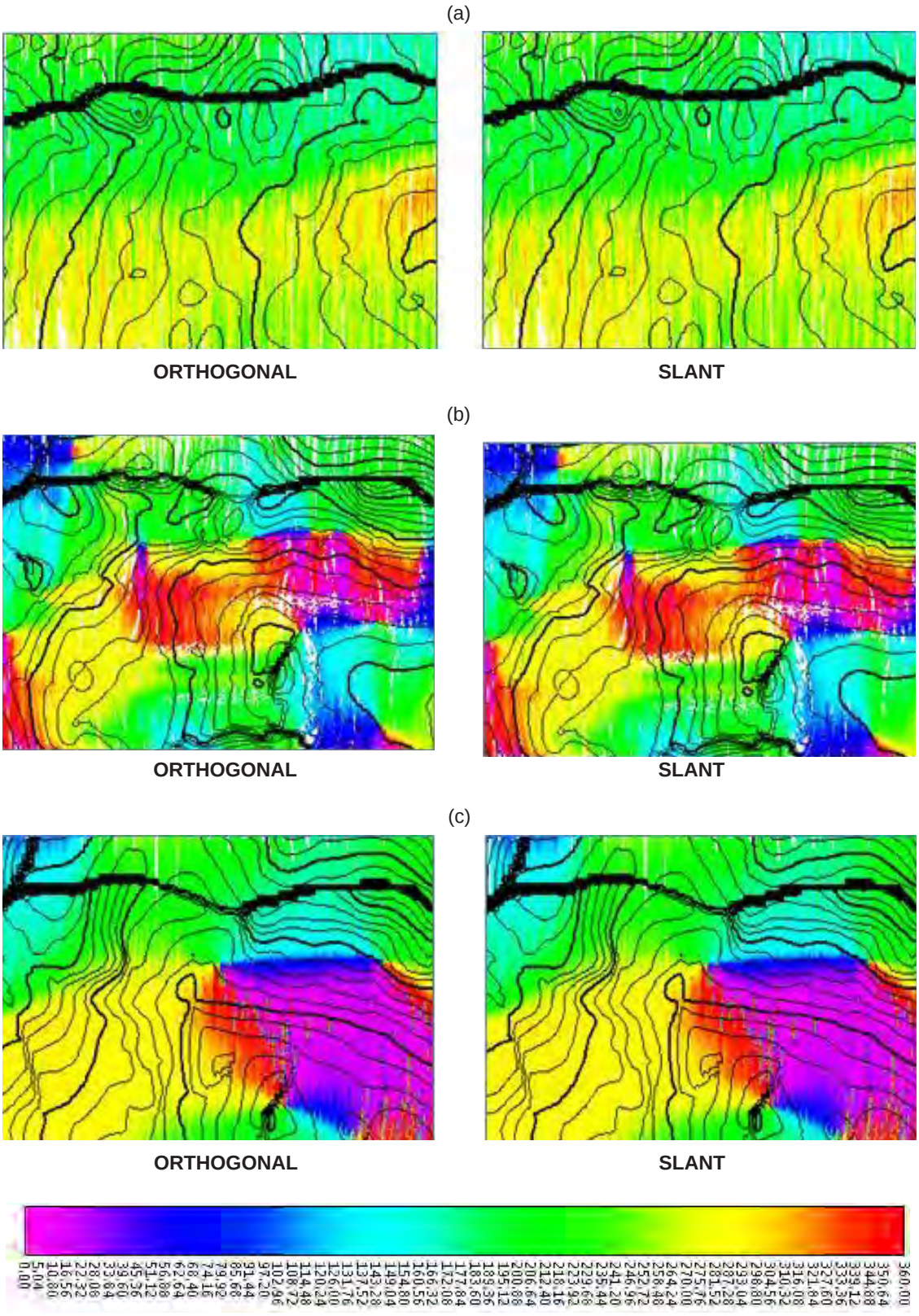

Figure 13
CDP – CRP displacement azimuth: (a) Horizon 1, (b) Horizon 2, (c) Horizon 3; it can be seen that the distribution of CDP-CRP displacement azimuth for the deeper horizon is more complicated.

Offset Raytracing

The following attributes are related to the normal axis of the group and phase velocity vectors, a shift occurs between CDP and CRP as shown in Figure 1, when the vectors intersect with the layer boundary planes. This led to a difference between the group and phase velocities. The image in Figure 11, shows a shift along the geological structure, such as a fault extending WE. Additionally, the deeper the shift value, the greater the shift. The offset raytracing, such as in the normal case also met the azimuth of CDP-CRP shifting. In the normal raytracing, the intersection points of the normal with the bedding boundary plane were observed. In Figure 12, the attribute was different from the normal azimuth, because normal raypath was perpendicular to each wavefront, both for the group and the phase velocity vectors. In this case, it attribute was controlled by geological structural conditions, similar to the previous ones. Concerning the existing diagram, there was no significant difference between orthogonal and slant modes.

Discussion

Normal or offset raytracing show a shift due to side-slip velocity as stated in Equation 9. The process was determined by the value of anisotropic constant in Table 1, where the higher the side-slip velocity value, the greater the shift. This also implied the greater the difference between group and phase velocities. The patterns from the distribution of normal and offset shifts showed that these were strongly influenced by geological structure. Some examples promoted large shifts in CDP-CRP position, specifically lateral dissonance boundary areas. This enabled diffraction to occur at the fault plane, resulting in seismic wave phase change (Ronoatmojo et al, 2010, Ronoatmojo and Burhannudinnur, 2018). Therefore, the seismic waves are rotated, and increase side-slip velocity in both normal and CDP-CRP displacement azimuth, as shown in Figures 10 and 12.

The maximum incident angle attribute in Figure 8, showed similar pattern in the normal and CD - CRP shifts in Figures 9 and 11, respectively. This showed that the higher the maximum incident angle, the greater the shift. Therefore, the maximum incident angle and the two shift attributes were controlled by the geological structure. On the anticline ridges waves were relatively diffracted and spread out, causing the displacement value to be higher on synclines, where there is a concentration of waves.

The entire attributes showed the medium was both anisotropic and heterogeneous. The heterogeneity was ineffective when sampled with slanted mode. The process was initially expected to enhance wave rotation pattern, but after observing the azimuth of the existing shift, it was not much different, compared to the orthogonal mode. The expected improvement was observed when forward modeling was carried out to evaluate the shift magnitude, before applying the depth migration.

The complexity of the geological structure played a role in the direction of wave propagation, which led to the random distribution of side-slip velocity, and the rotation of seismic waves. Therefore, a forward modeling method, initially used to trace the seismic waves azimuth rotation was considered appropriate, before carrying out depth migration.

CONCLUSION

Side-slip velocity in anisotropic medium which causes a displacement vector of seismic wave propagation, was identified by the shifting of the ray-path perpendicular to wavefront from the original position. This was due to seismic wave propagation in anisotropic medium. The shifting magnitude was determined and influenced by the magnitude of side-slip velocity, and anisotropic constant of the medium. The bending of the ray-path, in terms of wave propagation, was influenced by the difference in acoustic impedance, and side-slip velocity. The resultant outcome was a shift and rotation of the ray-path azimuth, including a random shift in position when passing through a complex geological structure. These random changes were anticipated by modeling normal raytracing illumination and offset raytracing before the migration process was conducted. The anisotropy parameters is very helpful in directing the difference between group velocity and phase velocity, but when facing complex structural geology, its effectiveness needs to be supported by such modeling, so that the depth migration process can be optimal.

ACKNOWLEDGMENT

The authors are grateful to the Directorate of Research, Technology and Community Service (Ministry of Education and Culture) and Faculty of Earth Technology and Energy (Trisakti University), for providing the opportunity to carry out this research for the development of science and technology.

GLOSSARY OF TERMS

Symbol	Definition	Definition
CDP	Common depth point	none
CSP	Common shot point	none
P-wave	Primary / Longitudinal wave	none
S-wave	Secondary / Transversal wave	none
NMO	Normal move-out correction	msec
$V(\phi)$	Velocity group	m/sec
$V(\theta)$	Phase velocity	m/sec
ϕ	Group angle	degree
θ	Phase angle	degree
ω	Phase	degree
v_{az}	Phase velocity along z axis	m/sec
v_{ax}	Phase velocity along x-axis	m/sec
VSP	Vertical seismic profile	none
PSDM	Pre-stack depth migration	none
δ,ε	Anisotropic parameter	none
V_{p0}	Vertical velocity	m/sec
$V_{p\theta}$	Angle vertical velocity	m/sec

REFERENCES

Bachman, R.T. (1979). *Acoustic anisotropy in marine sediments and sedimentary rocks*, Journal of Geophysical Research, 84, B13, p.7661-7663

Berkhout, A.J. (1984). *Seismic migration*, Elsevier Publ., Amsterdam

Blangy, J.P. (1994). *AVO in transversely isotropic media- an overview*, Geophysics 59, p. 775-781

Byun, B.S. (1984). *Seismic parameters for transversely isotropic media, in Velocity analysis on multichannel seismic data*, Byun, B.S., ed., Society of Exploration Geophysics, Tulsa, 84 -90

Claerbout, J.F. (1985). *Imaging the earth's interior,* Blackwell Sci. Publ., Oxford

Dellinger, J.A. (1991). *Anisotropic seismic wave propagation*, Stanford Univ. Ph.D dissertation, unpublished

Domenico , S.N. (1984) *Rock lithology and porosity determination from shear and compressional wave velocity*, Geophysics, 1188 - 1195

Jones, L.E.A and Wang, H.F. (1981). *Ultrasonic velocities in Cretaceous shales from the Williston basin*, Geophysics, 46, 288-297

Levin, F.K. (1978). *The reflection, refraction, and diffraction of waves in media with an elliptical velocity dependence*, Geophysics, 43, 528 – 537

Mayne, W.H. (1962). Common reflection point horizontal stacking techniques, Geophysics, 27, 927-938

Ronoatmojo, I.S. and Burhannudinnur (2018). *Anisotropic properties identification of Naintupo Formation, Tabul Formation and Tarakan Formation (Tarakan Sub-Basin) using anisotropic parameters determination method from P-wave seismic diffraction function*, IOP Conference Series: Earth and Environmental Science Vol.212 (2018) 012075 IOP Publishing doi:10.1088/1755-1315/212/1/012075, p.1- 11

Ronoatmojo, I.S., Santoso, D., Sanny ,T.A., and Fatkhan. (2010). *Seismic P-wave diffraction modeling to determine anisotropy parameters in VTI medium*, Proceeding of the SEG/Denver 2010 Annual Meeting, The Society of Exploration Geophysicist , Denver

Ruger, A. (1997). *P-wave reflection coefficients for transversely isotropic models with vertical and horizontal axis of symmetri,* Geophysics, 62, 713-722

Sheriff, R.E. (2002). *Encyclopedia of Geophysics*, Tulsa

Sheriff, R.E., and Geldart, L.P. (1995). Exploration Seismology, 2nd Edition, Cambridge University Press

Taner,M.T., Koehler, F., and Alhilali, K.A. (1974). *Estimation and correction of near surface time anomalies*, Geophysics, 441-463

Ullemeyer, K., Siegesmund, S., Rasolofosaon, P.N.J., and Behrmann, J.H. (2006). "Experimental and Texture-Derived P-Wave Anisotropy of Principal Rocks from the TRANSALP Traverse: An Aid for the Interpretation of Seismic Field Data." Tectonophysics 414(1-4): 97–116.

The influence of vside-slip velocity

by Imam Setiaji Ronoatmojo

Submission date: 11-Sep-2024 04:39PM (UTC+0700)
Submission ID: 2434701352
File name: 1620-3244-1-PB-1_the_influence_of_side-slip.pdf (2.64M)
Word count: 4815
Character count: 28145

Scientific Contributions Oil & Gas, Vol. 47. No. 2, August: 143-158
SCIENTIFIC CONTRIBUTIONS OIL AND GAS
Testing Center for Oil and Gas
LEMIGAS
Journal Homepage:http://www.journal.lemigas.esdm.go.id
ISSN: 2089-3361, e-ISSN: 2541-0520

The Influence of Side-Slip Velocity on Subsurface Displacement

Imam Setiaji Ronoatmojo, Muhammad Burhannudinnur, Yarra Sutadiwiria and Dewi Syavitri

Universitas Trisakti
Kyai Tapa 1 Street, Jakarta, Indonesia

Corresponding author: aji.rono@trisakti.ac.id

Manuscript received: June 26th, 2024; Revised: July 26th, 2024
Approved: July 29th, 2024; Available online: July 31st, 2024

ABSTRACT - This research aimed to determine the influence of side-slip velocity on subsurface displacement during seismic data acquisition. Anisotropy constants were used to determine the depth migration process before stack, which showed inadequate results after data validation. Therefore, the forward modeling of a medium, which comprised anisotropy constants of normal and offset raytracing was conducted to address this problem. The configuration of source to receiver were orthogonal and slant. The results showed that the migration process failed to resolve the geological structures of the position shifting. The configuration of source to receiver were orthogonal and slant. The results show the better continuity of slant and the influence of complex geological structures controls the position shifting, which could not be resolved by the migration process. It could be seen from the random distribution of the normal shift of group velocity and phase velocity, as well as the CDP – CRP shift. It produced wave azimuth rotation in a discontinuity plane, such as fault and anticline ridge. This azimuth rotation was strongly suspected to cause inaccurate anisotropy constants implementation in pre-stack depth migration process.

Keywords: side-slip velocity, anisotropy constants, migration, normal displacement, CDP-CRP displacement.

How to cite this article:

Imam Setiaji Ronoatmojo, Muhammad Burhannudinnur, Yarra Sutadiwiria and Dewi Syavitri, 2024, The Influence of Side-Slip Velocity on Subsurface Displacement, Scientific Contributions Oil and Gas, 47 (2) pp. 143-158. DOI.org/10.29017/SCOG.47.2.1620.

INTRODUCTION

Seismic anisotropy is associated with velocity variations in pre-stack depth migration. This led to the issue of deviated result in time to depth domain transformation, specifically observed when validated with well data. The current research investigated the effect of anisotropic medium on wave velocity, despite the varying constants. Anisotropic medium was designed by using the constants to determine the actual response. Additionally, this was modeled in respect to the previous seismic data interpretation, conducted in Naintupo, Tabul, and Tarakan Formations, found at approximately 1,000 to 3,000 meters beneath the earth surface. The thick intercalation of sand-shale lithology produced anisotropic tendencies, due to the presence of bedding planes. Anisotropic occurrence in sedimentary rocks is related to the sedimentation process of different layers, strata or minerals with various grain sizes. These secondary structures or macro-scale features of rocks were also defined as discontinuities. The influence of anisotropic medium properties was reflected as the difference between group and phase velocities (Ronoatmojo and Burhannudinnur, 2018).

Anisotropy of materials such as the earth must be taken into account during data acquisition and interpretation. According to Sheriff (2002) seismic

anisotropy is defined as seismic velocity variation depending on the propagating direction of either P- or S- waves or polarization (for S-waves). Velocity as a physical parameter plays an important role in seismic exploration, as well as defines anisotropic properties. The estimation accuracy is important, because velocity is a critical parameter that influences the quality of near-surface distortion correction (Taner et.al, 1974), multi-fold data processing (Mayne, 1962) and seismic data migration (Berkhout, 1984; Claerbout, 1985). Physical properties also has an impact on the interval velocity estimation, including the transformation of time to depth using Dix formula and tomographic methods. Therefore, adequate knowledge of lithology and stratigraphy is needed, to observe seismic wave propagating through any anisotropic medium (Domenico, 1984).

Material heterogeneity depends on the difference in physical properties at various positions, particularly when anisotropic nature of matter is manifested as varying wave velocity orientations in various directions. Therefore, the medium is isotropic and homogeneous, contradicting the fact that it is anisotropic and heterogeneous. This depends on the primary arrangement of the rock-forming minerals referred to as microscopic packing (Ullemeyer et al, 2006). Anisotropic tendencies in seismic exploration were observed as the differences in velocity values in the vertical and horizontal directions. These differences tend to appear, specifically when far offsets are used.

In 1932, McCollum and Snell conducted research and reported that the horizontal P-wave velocity of the Lorraine shale in Canada was 1.4 times the vertical P-wave velocity (Levin, 1978). Similarly, various research on anisotropy conducted since the 1950s stated that the tendencies occurred when the thickness of the layer was less than the seismic wavelength propagated in the medium (Postma, 1955; Dellinger, 1991). Meanwhile, evidence of intrinsic anisotropy was obtained from the laboratory analyses of several rock samples related to the change in pressure beneath the surface (Nur, 1969; Dellinger, 1991). Bachman (1979), found transverse isotropy in cores originating from deep sea drilling. Jones and Wang (1981), made similar observations in cores from the Williston Basin, North Dakota.

The application of anisotropic properties was ignored until the 1980s, because most seismic data were recorded in respect to near to medium offsets, even though the medium was not isotropic. It was observed that the use of far offset data, specifically for anisotropic media during NMO or normal move-out process, led to difficulties in obtaining the accurate velocity correction. Another influence of anisotropic properties was observed during migration, where far offset travel time with an angle greater than 40^0 led to energy shifting from the original path to another position, as shown in Figure 1. This refers to the tangent point position of wavefront (Dellinger, 1991).

Anisotropic assumptions such as AVO, or amplitude versus offset analysis, must be taken into account, during seismic data interpretation. Meanwhile, Blangy (1994), and Ruger (1998), made certain corrections to the Aki-Richard equation by inserting anisotropic parameters. The constant estimation could be determined either directly or indirectly. Direct and indirect observations were carried out using VSP data, and reflection or diffraction function, respectively (Ronoatmojo et al, 2010). Diffraction is henomenon of energy scattering at discontinuity plane, so that transmission waves from sources below surface, can be used to determine anisotropic constants. This is done if there are no wells penetrating the area.

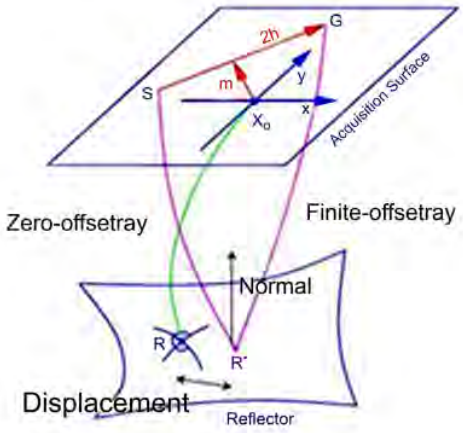

Figure 1
CDP – CRP displacement.

The phase velocity denoted as simply means that the distance traveled per unit time is in the constant phase position, such as in the trough or peak of wave (Sheriff and Geldart, 1995). The process is not similar to the group velocity, which is velocity with energy

propagates from one point to another. For example, in Figure 2, the group velocity $= \frac{\Delta x}{\Delta t_g}$

in waves series. It is described as velocity obtained from the slope of the pulse envelopes top (ABC and AB'C curves). The phase velocity was described as velocity obtained from the slope of a line representing similar phase state, equivalent to $\frac{\Delta x}{\Delta t_p}$. When a pulse is decomposed into frequency components in a Fourier spectrum, the phase and group velocities tend to be similar for all frequency values. Variations in phase velocity relative to the frequency, changes the pulse shape, and the group velocity. The relationship between group and phase velocities in the dispersive medium is expressed in Equation (1):

$$V(\emptyset) = V(\theta) - \lambda \frac{dV(\theta)}{d\lambda} = V(\theta) + \omega \frac{dV(\theta)}{d\omega} \quad (1)$$

where $\frac{dV(\theta)}{d\lambda}$ and $\frac{dV(\theta)}{d\omega}$ are the phase velocity change in varying wavelengths or frequencies. Assuming the phase velocity decreases as the frequency increases, the value obtained would be greater than the group velocity as shown in Figure 2. The phase velocity is less than the group velocity, when it increases with increasing frequency. Furthermore, the difference between these velocities in a dispersive medium was showed by the change in pulse shape. This is caused by alterations in phase velocity with respect to frequency variations. The process does not always occur in every medium, and important in differentiating the occurrence of anisotropy.

In anisotropic medium, the relationship between group $V(\varphi)$ and phase velocities $V(\theta)$ is expressed in Equation (2):

$$V(\phi)^2 = V(\theta)^2 + \left(\frac{dV(\theta)}{d(\theta)}\right)^2 \quad (2)$$

The difference in Equation 2 was based on variations in phase velocity in respect to wavefront normal, where θ is the phase angle and ϕ the group angle. However, the difference between the group and phase velocities in anisotropic medium determines the magnitude of the position shifting beneath the surface. The larger the difference, the greater the shifting, or the more anisotropic the medium, the further the position of a point would be shifted from the origin.

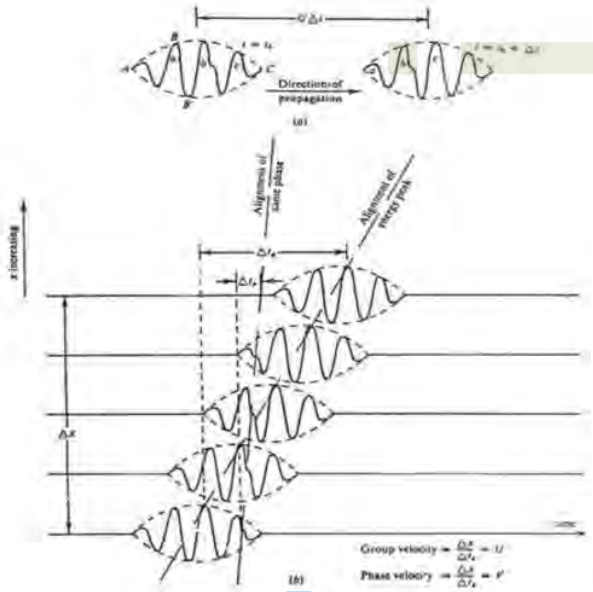

Figure 2
Group and phase velocities in a dispersive medium (Sheriff and Geldart, 1995).

Preliminary investigation on the relationship between group and phase velocities, alongside technological advances regarding the use of data with large offsets and multi azimuth, led to the problem of velocity anisotropy. An overview of the geometry between group and phase velocities is needed to understand position displacement. Byun (1984; 2000), conducted research on the elliptic nature of the raypath velocity associated with the group velocity. Generally, assuming a medium is anisotropic, velocity in the direction of wave propagation or seismic energy would differ from the one in the perpendicular wavefront The geometry described by Byun (1984) in Figure 3, shows that α is the angle formed by the group trajectory with the normal of the boundary plane, and γ is the angle between the axis and the normal of the boundary plane.

Wave surface is the points present in response to the source. Meanwhile, for anisotropic medium, this elliptical figure is determined using the ellipse equation:

$$V(\phi)^{-2} = v_{az}{}^{-2}cos^2\phi + v_{ax}{}^{-2}sin^2\phi \quad (3)$$

where and are the phase velocities along the z and x symmetry axes of the ellipse, while is the group (raypath) velocity at angle from the axis. Geometrically, the relationship and V(θ) could be defined using Equation (4):

$$V(\theta) = V(\phi)\cos(\phi - \theta) \quad (4)$$

assuming,

$$\tan\theta = \left(\frac{v_{az}}{v_{ax}}\right)^2 tan\phi \quad (5)$$

the relationship between V(θ) with and could be expressed as:

$$V(\theta)^2 = v_{az}{}^2cos^2\theta + v_{ax}{}^2sin^2\theta \quad (6)$$

The relationship between group and phase velocities in Figure 4, shows that if the normal of phase angle is squeezed with group angle, then the right-angled triangle SGF and SGF' would appear. Furthermore, phase and group velocity changes were detected in SGF and SGF' right-angled triangles, respectively. So by placing the group angle and phase angle on the same normal line axis, the geometric solution can be done more clearly. It can be seen that the group angle is always greater than the phase angle. It is understandable that the elliptical tendency results in decrease of the phase angle. So the stronger the anisotropy, the more phase angle shifts to the normal axis.

Considering SGF:

$$cos(\phi - \theta) = \frac{V(\theta)}{V(\phi)} \quad (7)$$

So,

$$cos(\phi - \theta) = \frac{V(\phi)}{\sqrt{V(\phi)^2 + \left(\frac{dV(\phi)}{d\phi}\right)^2}} \quad (8)$$

Regarding Equations (7) and (8), in anisotropic medium, the group velocity is greater than the phase velocity. It is the sum of the phase (perpendicular to wavefront) and side-slip velocity. Therefore, the greater the side-slip velocity , the more the position of subsurface point would be shifted, including increasing the elliptic factor of the group velocity. Assuming the equation used to determine the relationship between phase velocity and anisotropy parameter is substituted into Equation 9, it would produce a solution for measuring anisotropy parameter indirectly.

$$V(\theta) = \frac{V(\phi)^2}{\sqrt{V(\phi)^2 + \left(\frac{dV(\phi)}{d\phi}\right)^2}} \quad (9)$$

Thus, the above equation demonstrates goniometrically that the presence of anisotropic tendency will result in position shifting. The following work is to prove with an illumination modeling, which includes an anisotropic model and wave propagation which is considered by this model. It is done to find out the implication of structural complexity.

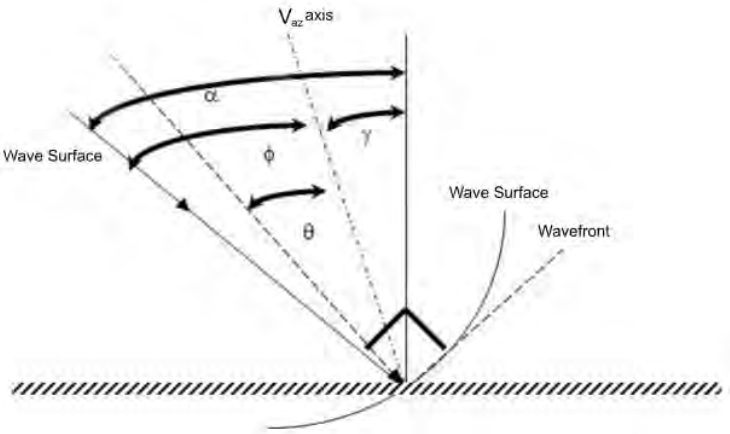

Figure 3
Geometry of raypath and phase in boundary plane (Byun, 1984).

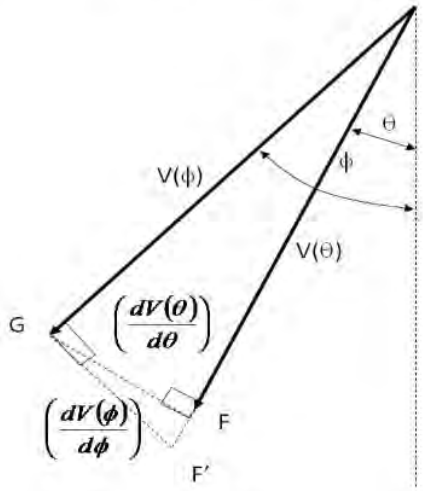

Figure 4
Geometry of group and phase velocities (Byun, 1984).

METHODOLOGY

Anisotropic properties could shift subsurface position as shown in Figure 1. However, during the migration process, this principle is not neglected, but it resulting in inaccurate position of the seismic to the well data. Therefore in this research, it was began from a forward modeling which is generated from three-dimensional seismic data, built from Pre-stack Depth Migration (PSDM). Anisotropic parameters were determined from VSP of three existing markers, whose constants were calculated based on the average velocity of each. This was considered as vertical (), and angle velocity () for the far offset.

Table 1
Anisotropy constants (and)

Marker	δ		ε	
	Well-A	Well-B	Well-A	Well-B
1	0.23	0.4	0.18	0.38
2	0.31	0.52	0.31	0.49
3	0.35	0.63	0.36	0.67

The results of the previously interpreted seismic data were used as model input for carrying out illumination work on wave propagation. This was realized by entering anisotropy constant value as a factor that would correct the group velocity. Theoretically, anisotropic parameter was applied based on the geometry of the material, including velocity function, phase and wavelength. It failed to consider the vertical resolution, due to the large thickness of the inter horizons, which exceeded the existing resolution. However, the lateral resolution was calculated based on the Fresnel zone. After wave travel time was obtained, the position of each subsurface data set (CDP gather) was determined in respect to the depth value. This was also defined through the layer boundary plane, represented by the horizon. Acquisition lay-out was simulated orthogonally and slanted, to compare several items related to fold distribution, offset orientation and azimuth. The complete sequence of the work flow is shown in Figure 5.

The geological structure examined in Figure 6, is a giant W-E fault structure that extends to an W-E anticline ridge. This small fault is perpendicular to the giant W-E structure with N-S orientation. Northward to the anticline ridge, is a homocline with a dip. Meanwhile, a syncline valley is found towards the south. This interesting model, has stratigraphic anisotropy constants, as well as a fairly complex geological structure, which have an impact in the bending of wave propagation.

The two types of layouts were designed orthogonally and slanted, with each receiver lines oriented in N-S direction. Therefore, it was crossed perpendicularly through most of the structures, except for N-S. In Figure 7a, the orthogonal layout, referred to as the source line orientation (W-E) is perpendicular to the receiver line, where SLI (Source Line Interval) and RLI (Receiver Line Interval) are 800 meters and 300 meters, respectively, and the number of active channels is 2.016 units. Meanwhile, the other layout is slanted as shown in Figure 7b with the source line orientation (N-S) forming an oblique angle with the receiver line, where SLI and RLI is 800 meters and 250 meters, respectively, and the number of active channels is 2.000 units.

The slant mode was used to determine, whether the source line designed at an angle to the receiver, influences shifting continuity. CDP is subsurface point, reflected at the layer boundary plane, but due to anisotropic characteristic, it was shifted by the slide slip velocity, and was referred to as CDP – CRP displacement. The difference between orthogonal and slant modes were observed in Figures 8a and b, where the design in the cross section, showed the richer data filling in the slant mode. In this case, the slant mode offsets filling more in the existing vertical grids, and when combined with the cross-line offsets, data continuities would be better. This is important to strengthen the coherency of the data to be sampled. However, there is need for further investigation to ascertain whether data continuity would affect anisotropic problems.

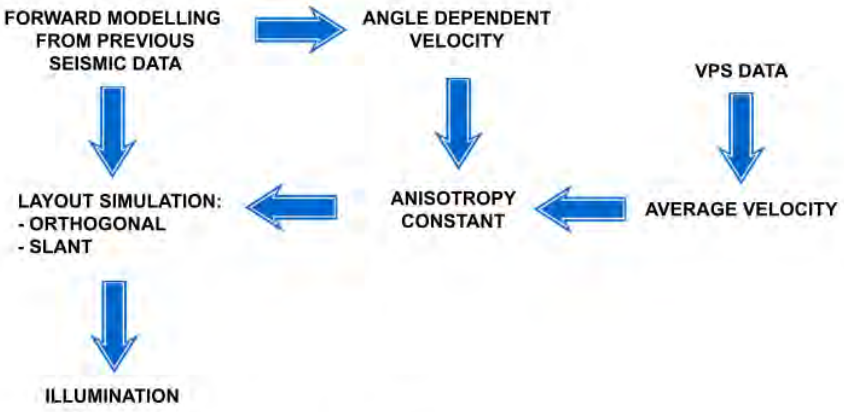

Figure 5
Workflow.

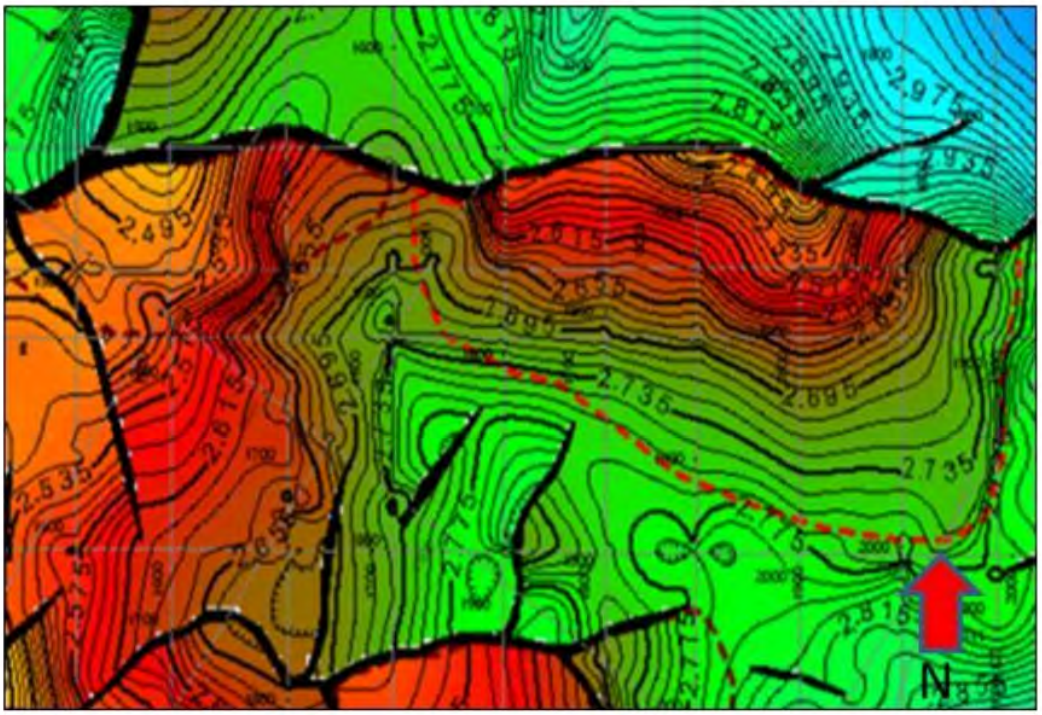

Figure 6
Geological structure of the model to be studied.

(a)

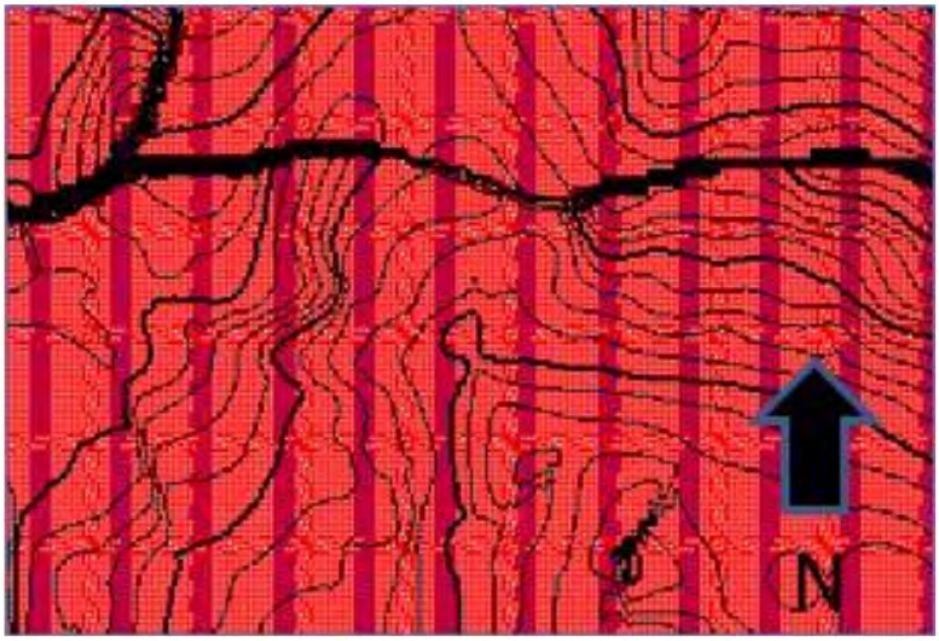

Scientific Contributions Oil & Gas, Vol. 47. No. 2, August 2024: 143 - 158

(b)

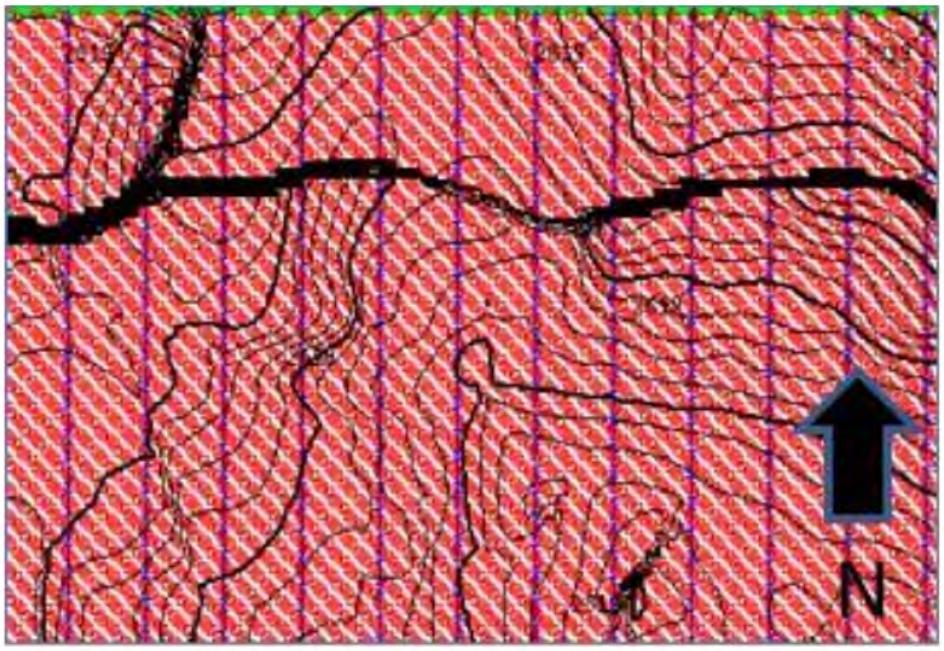

Figure 7
Lay-out: (a) orthogonal, (b) slant which is simulated to describe the ray-path configuration during data acquisition.

(a)

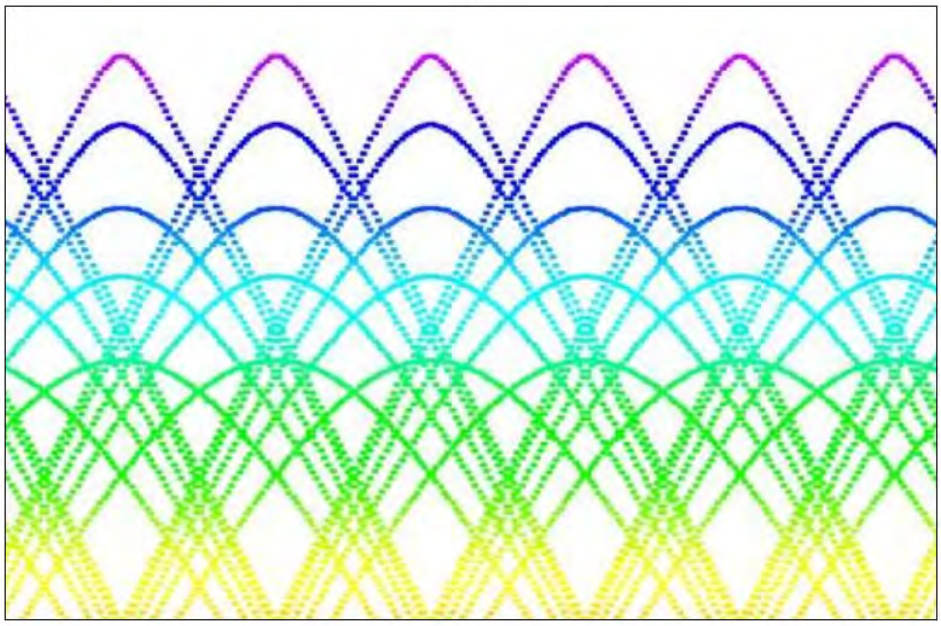

(b)

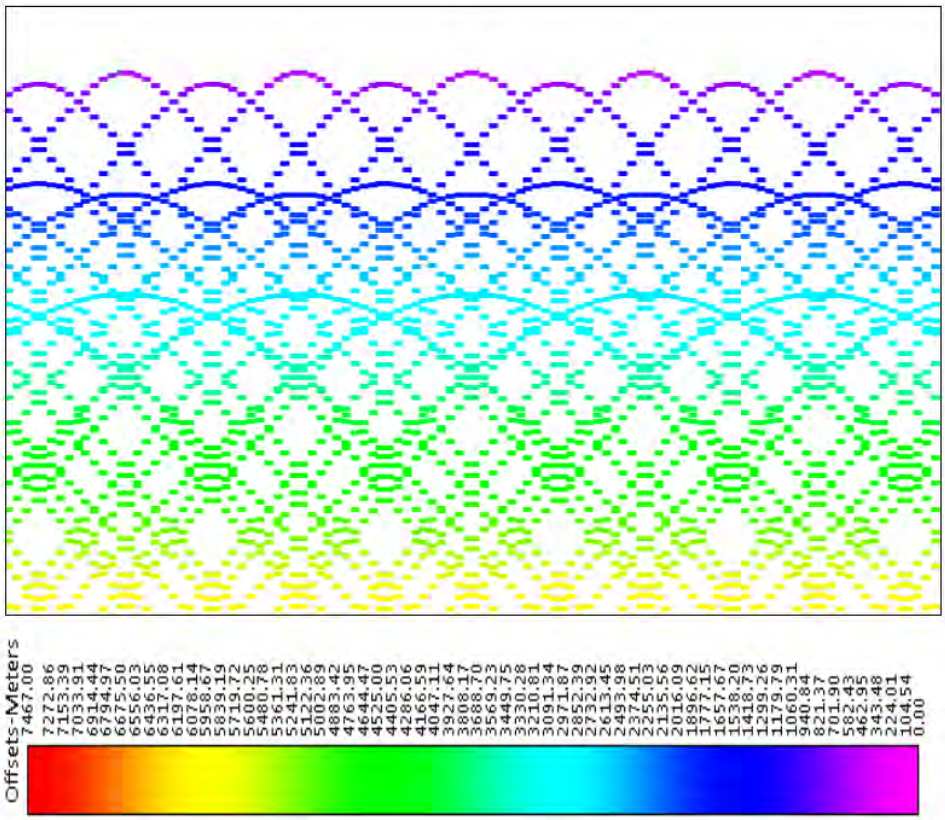

Figure 8
Lay-out in-line section: (a) orthogonal, (b) slant which shows the different configurations of the offset distribution transversely with the color indicating depth where the red color on the color bar scale showing the longest offset.

RESULT AND DISCUSSION

Normal Raytracing

After illumination, the maximum incident angle distribution was obtained from each horizon. Additionally, the group angle was formed with respect to the normal of the bedding boundary plane. The distribution obtained for each horizon showed that the value of the maximum incident angle for the shallowest horizon, was greater than the maximum incident angle for the deeper horizon. Meanwhile, the image of the slant mode was slightly different from the orthogonal. The faults and anticline ridges had a tendency to increase the value of the maximum incident angle as shown in Figure 9.

The normal of a layer boundary plane, is assumed to be the normal of group angle, while the normal of phase angle is a line perpendicular to wavefront. Figure 9 shows that in respect to the shifting between group and phase normal, the highest shift was larger for faults and anticline ridges, while synclines had lower shift. Furthermore, the complex features were observed in the deeper Horizons 2 and 3, caused by the raypath model, which was not bent above Horizon 1.

The shift was also observed in the azimuth direction as shown in Figure 10. When combined with the previous attributes, it was used to explain the vector of normal shifting. Additionally, the influence of the geological structure depended on the azimuth distribution.

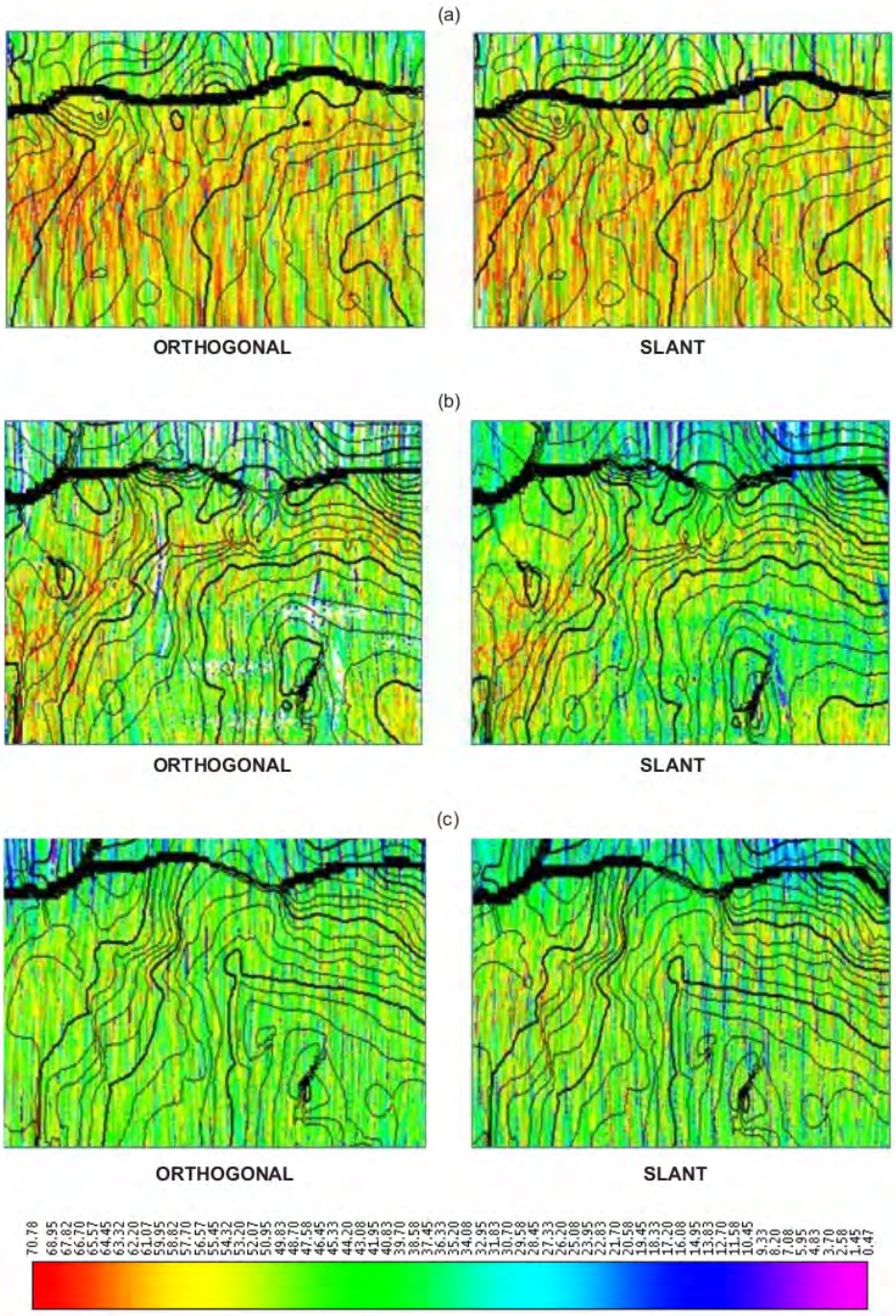

Figure 9
Maximum incident angle: (a) Horizon 1, (b) Horizon 2, (c) Horizon 3; it can be seen that the distribution of maximum incident angles for the shallower horizon is higher.

 | DOI.org/10.29017/SCOG.47.2.1620

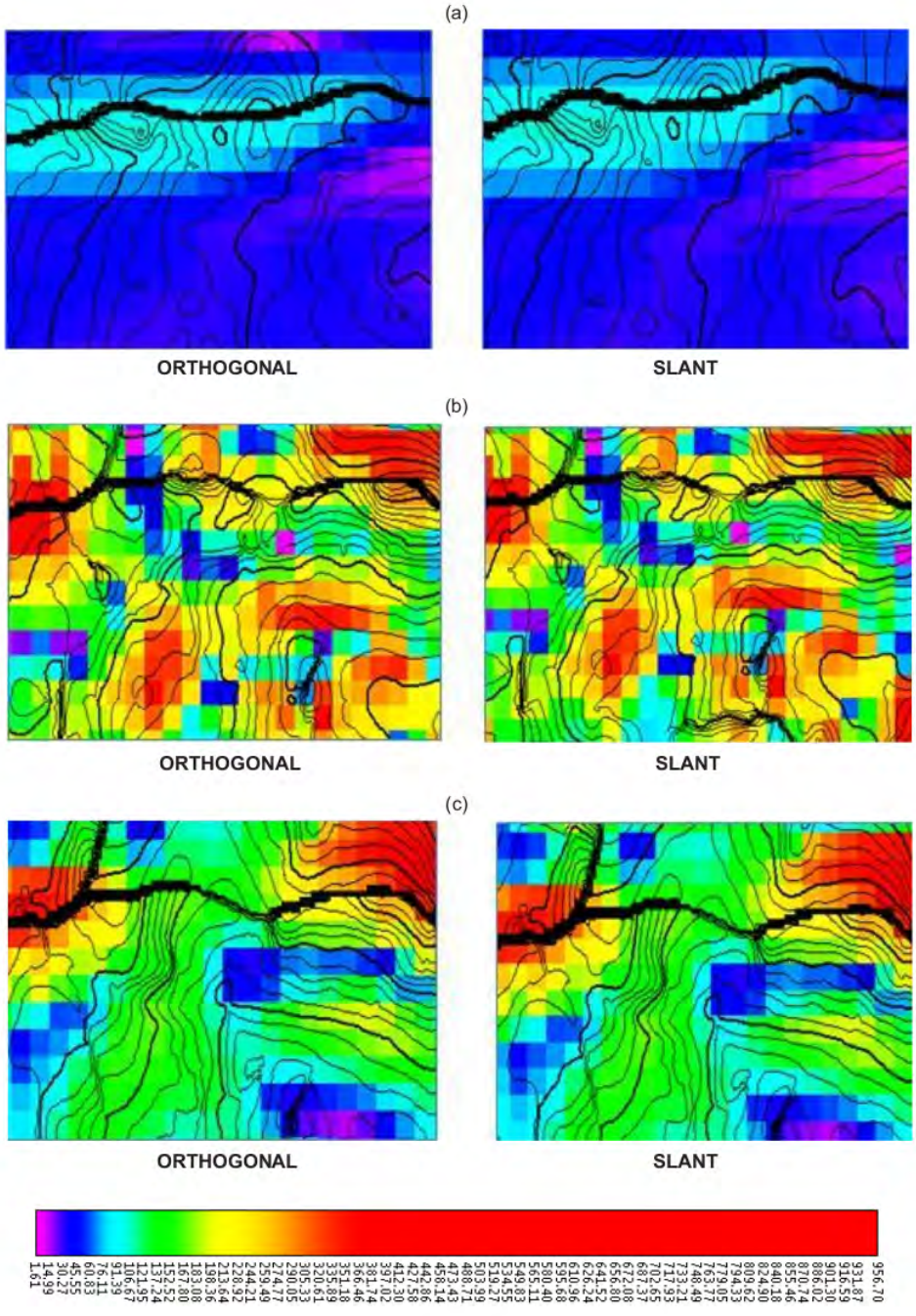

Figure 10
Normal displacement: (a) Horizon 1, (b) Horizon 2, (c) Horizon 3; it can be seen that the distribution of normal displacement for the shallower horizon is lower.

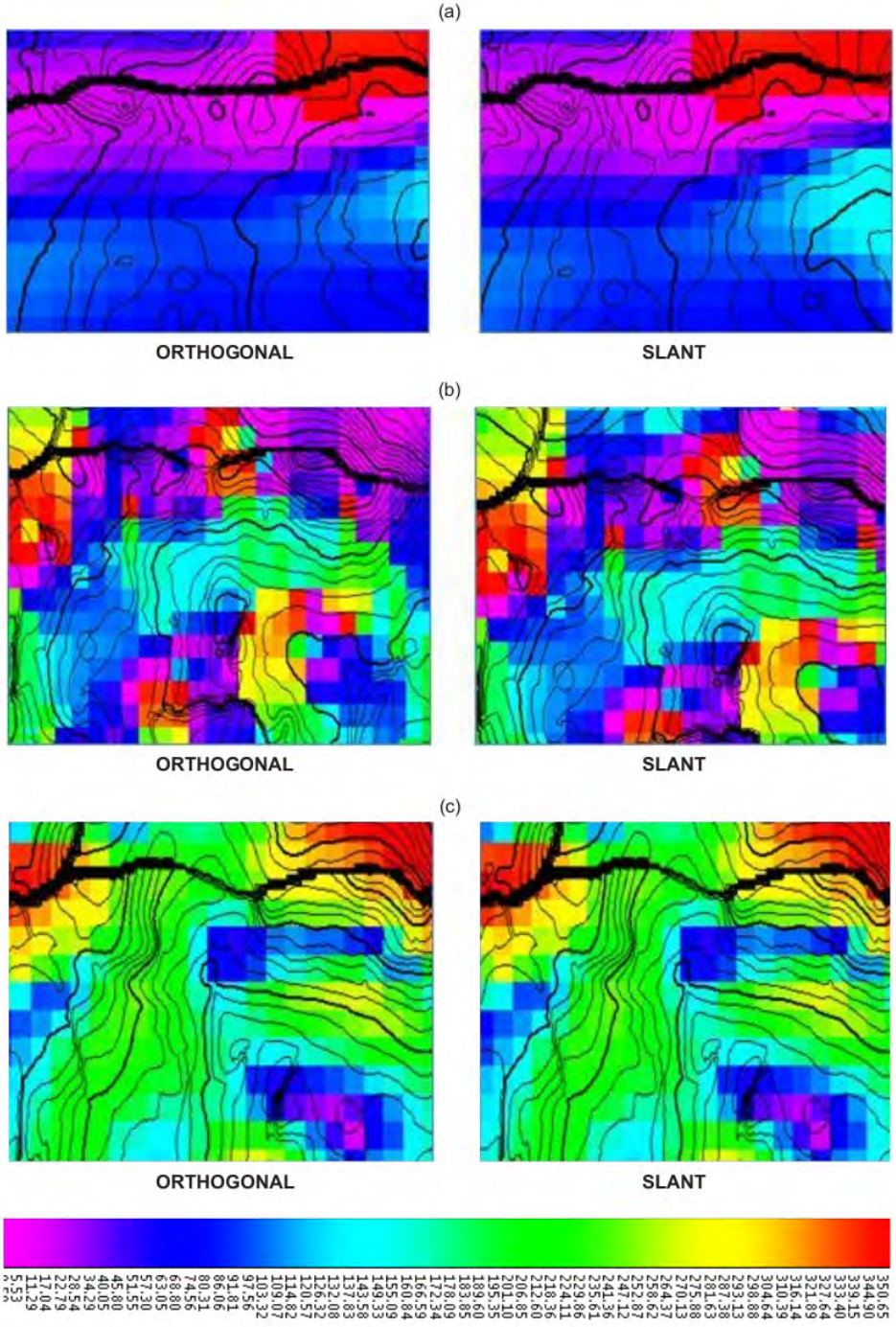

Figure 11
Normal azimuth: (a) Horizon 1, (b) Horizon 2, (c) Horizon 3; it can be seen that the distribution of normal azimuth for the shallower horizon is lower.

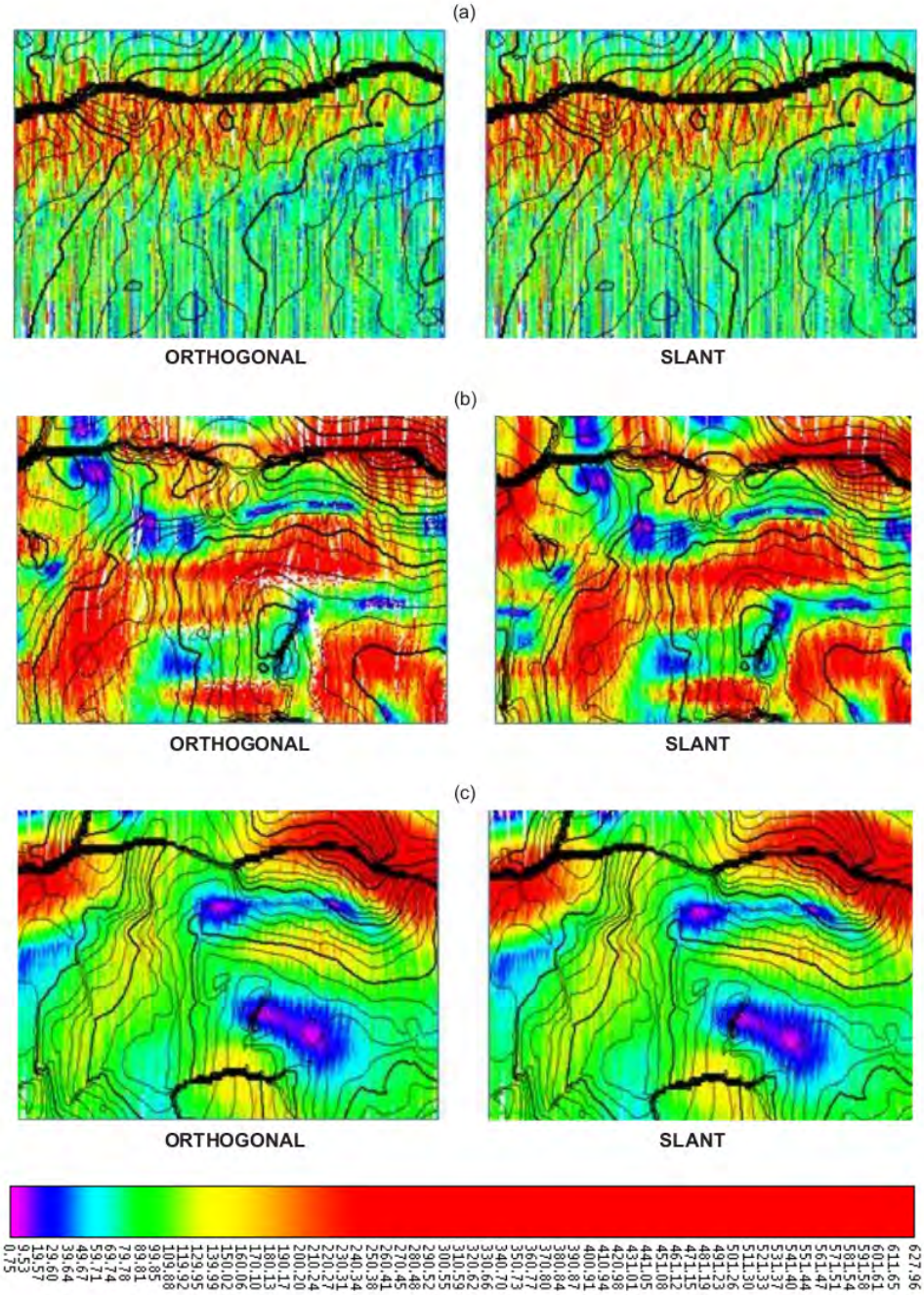

Figure 12
CDP – CRP displacement: (a) Horizon 1, (b) Horizon 2, (c) Horizon 3; it can be seen that the distribution of CDP-CRP displacement for the deeper horizon is more complicated

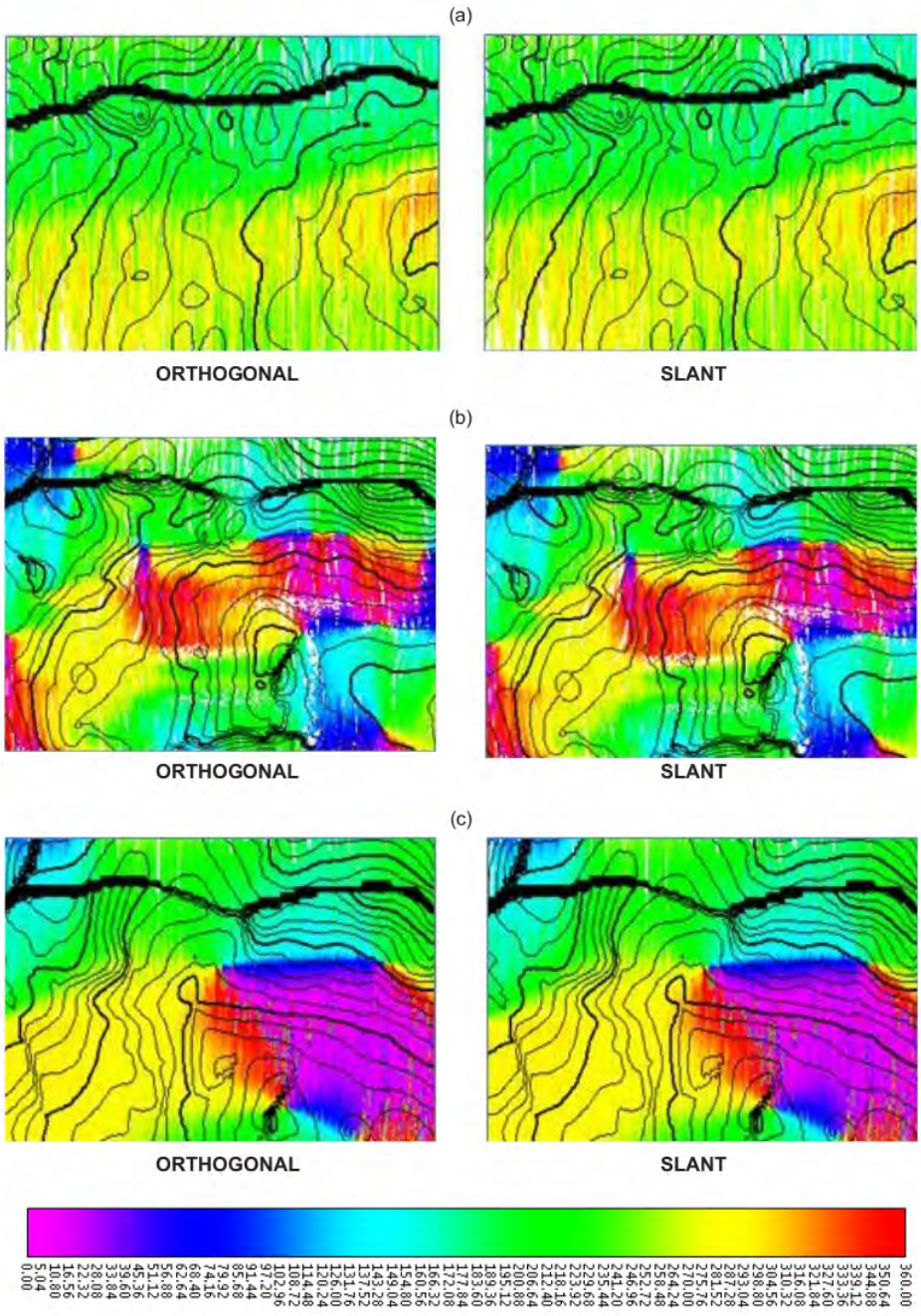

Figure 13
CDP – CRP displacement azimuth: (a) Horizon 1, (b) Horizon 2, (c) Horizon 3; it can be seen that the distribution of CDP-CRP displacement azimuth for the deeper horizon is more complicated.

Offset Raytracing

The following attributes are related to the normal axis of the group and phase velocity vectors, a shift occurs between CDP and CRP as shown in Figure 1, when the vectors intersect with the layer boundary planes. This led to a difference between the group and phase velocities. The image in Figure 11, shows a shift along the geological structure, such as a fault extending WE. Additionally, the deeper the shift value, the greater the shift. The offset raytracing, such as in the normal case also met the azimuth of CDP-CRP shifting. In the normal raytracing, the intersection points of the normal with the bedding boundary plane were observed. In Figure 12, the attribute was different from the normal azimuth, because normal raypath was perpendicular to each wavefront, both for the group and the phase velocity vectors. In this case, it attribute was controlled by geological structural conditions, similar to the previous ones. Concerning the existing diagram, there was no significant difference between orthogonal and slant modes.

Discussion

Normal or offset raytracing show a shift due to side-slip velocity as stated in Equation 9. The process was determined by the value of anisotropic constant in Table 1, where the higher the side-slip velocity value, the greater the shift. This also implied the greater the difference between group and phase velocities. The patterns from the distribution of normal and offset shifts showed that these were strongly influenced by geological structure. Some examples promoted large shifts in CDP-CRP position, specifically lateral dissonance boundary areas. This enabled diffraction to occur at the fault plane, resulting in seismic wave phase change (Ronoatmojo et al, 2010, Ronoatmojo and Burhannudinnur, 2018). Therefore, the seismic waves are rotated, and increase side-slip velocity in both normal and CDP-CRP displacement azimuth, as shown in Figures 10 and 12.

The maximum incident angle attribute in Figure 8, showed similar pattern in the normal and CD - CRP shifts in Figures 9 and 11, respectively. This showed that the higher the maximum incident angle, the greater the shift. Therefore, the maximum incident angle and the two shift attributes were controlled by the geological structure. On the anticline ridges waves were relatively diffracted and spread out, causing the displacement value to be higher on synclines, where there is a concentration of waves.

The entire attributes showed the medium was both anisotropic and heterogeneous. The heterogeneity was ineffective when sampled with slanted mode. The process was initially expected to enhance wave rotation pattern, but after observing the azimuth of the existing shift, it was not much different, compared to the orthogonal mode. The expected improvement was observed when forward modeling was carried out to evaluate the shift magnitude, before applying the depth migration.

The complexity of the geological structure played a role in the direction of wave propagation, which led to the random distribution of side-slip velocity, and the rotation of seismic waves. Therefore, a forward modeling method, initially used to trace the seismic waves azimuth rotation was considered appropriate, before carrying out depth migration.

CONCLUSION

Side-slip velocity in anisotropic medium which causes a displacement vector of seismic wave propagation, was identified by the shifting of the ray-path perpendicular to wavefront from the original position. This was due to seismic wave propagation in anisotropic medium. The shifting magnitude was determined and influenced by the magnitude of side-slip velocity, and anisotropic constant of the medium. The bending of the ray-path, in terms of wave propagation, was influenced by the difference in acoustic impedance, and side-slip velocity. The resultant outcome was a shift and rotation of the ray-path azimuth, including a random shift in position when passing through a complex geological structure. These random changes were anticipated by modeling normal raytracing illumination and offset raytracing before the migration process was conducted. The anisotropy parameters is very helpful in directing the difference between group velocity and phase velocity, but when facing complex structural geology, its effectiveness needs to be supported by such modeling, so that the depth migration process can be optimal.

ACKNOWLEDGMENT

The authors are grateful to the Directorate of Research, Technology and Community Service (Ministry of Education and Culture) and Faculty of Earth Technology and Energy (Trisakti University), for providing the opportunity to carry out this research for the development of science and technology.

GLOSSARY OF TERMS

Symbol	Definition	Definition
CDP	Common depth point	none
CSP	Common shot point	none
P-wave	Primary / Longitudinal wave	none
S-wave	Secondary / Transversal wave	none
NMO	Normal move-out correction	msec
$V(\phi)$	Velocity group	m/sec
$V(\theta)$	Phase velocity	m/sec
ϕ	Group angle	degree
θ	Phase angle	degree
ω	Phase	degree
v_{az}	Phase velocity along z axis	m/sec
v_{ax}	Phase velocity along x-axis	m/sec
VSP	Vertical seismic profile	none
PSDM	Pre-stack depth migration	none
δ,ε	Anisotropic parameter	none
V_{p0}	Vertical velocity	m/sec
$V_{p\theta}$	Angle vertical velocity	m/sec

REFERENCES

Bachman, R.T. (1979). *Acoustic anisotropy in marine sediments and sedimentary rocks*, Journal of Geophysical Research, 84, B13, p.7661-7663

Berkhout, A.J. (1984). *Seismic migration*, Elsevier Publ., Amsterdam

Blangy, J.P. (1994). *AVO in transversely isotropic media- an overview*, Geophysics 59, p. 775-781

Byun, B.S. (1984). *Seismic parameters for transversely isotropic media, in Velocity analysis on multichannel seismic data,* Byun, B.S., ed., Society of Exploration Geophysics, Tulsa, 84 -90

Claerbout, J.F. (1985). *Imaging the earth's interior,* Blackwell Sci. Publ., Oxford

Dellinger, J.A. (1991). *Anisotropic seismic wave propagation*, Stanford Univ. Ph.D dissertation, unpublished

Domenico , S.N. (1984) *Rock lithology and porosity determination from shear and compressional wave velocity*, Geophysics, 1188 - 1195

Jones, L.E.A and Wang, H.F. (1981). *Ultrasonic velocities in Cretaceous shales from the Williston basin*, Geophysics, 46, 288-297

Levin, F.K. (1978). *The reflection, refraction, and diffraction of waves in media with an elliptical velocity dependence*, Geophysics, 43, 528 – 537

Mayne, W.H. (1962). Common reflection point horizontal stacking techniques, Geophysics, 27, 927-938

Ronoatmojo, I.S. and Burhannudinnur (2018). *Anisotropic properties identification of Naintupo Formation, Tabul Formation and Tarakan Formation (Tarakan Sub-Basin) using anisotropic parameters determination method from P-wave seismic diffraction function*, IOP Conference Series: Earth and Environmental Science Vol.212 (2018) 012075 IOP Publishing doi:10.1088/1755-1315/212/1/012075, p.1- 11

Ronoatmojo, I.S., Santoso, D., Sanny ,T.A., and Fatkhan. (2010). *Seismic P-wave diffraction modeling to determine anisotropy parameters in VTI medium*, Proceeding of the SEG/Denver 2010 Annual Meeting, The Society of Exploration Geophysicist , Denver

Ruger, A. (1997). *P-wave reflection coefficients for transversely isotropic models with vertical and horizontal axis of symmetri*, Geophysics, 62, 713-722

Sheriff, R.E. (2002). *Encyclopedia of Geophysics*, Tulsa

Sheriff, R.E., and Geldart, L.P. (1995). Exploration Seismology, 2nd Edition, Cambridge University Press

Taner,M.T., Koehler, F., and Alhilali, K.A. (1974). *Estimation and correction of near surface time anomalies*, Geophysics, 441-463

Ullemeyer, K., Siegesmund, S., Rasolofosaon, P.N.J., and Behrmann, J.H. (2006). "Experimental and Texture-Derived P-Wave Anisotropy of Principal Rocks from the TRANSALP Traverse: An Aid for the Interpretation of Seismic Field Data." Tectonophysics 414(1-4): 97–116.

The influence of vside-slip velocity

ORIGINALITY REPORT

16%	14%	10%	4%
SIMILARITY INDEX	INTERNET SOURCES	PUBLICATIONS	STUDENT PAPERS

PRIMARY SOURCES

1	es.scribd.com Internet Source	6%
2	othes.univie.ac.at Internet Source	1%
3	www.karyailmiah.trisakti.ac.id Internet Source	1%
4	ntnuopen.ntnu.no Internet Source	1%
5	Klaus Helbig, Leon Thomsen. "75-plus years of anisotropy in exploration and reservoir seismics: A historical review of concepts and methods", GEOPHYSICS, 2005 Publication	1%
6	Submitted to School of Business and Management ITB Student Paper	1%
7	vdoc.pub Internet Source	1%

8	Imam S. Ronoatmojo. "Seismic P-wave diffraction modeling to determine anisotropy parameters in VTI medium", SEG Technical Program Expanded Abstracts, 2010 Publication	<1 %
9	joiv.org Internet Source	<1 %
10	www.researchgate.net Internet Source	<1 %
11	Submitted to University of Leeds Student Paper	<1 %
12	www.scribd.com Internet Source	<1 %
13	Darko Babunski, Jakup Berisha, Emil Zaev, Xhevahir Bajrami. "Application of Fuzzy Logic and PID Controller for Mobile Robot Navigation", 2020 9th Mediterranean Conference on Embedded Computing (MECO), 2020 Publication	<1 %
14	Yilmaz. "Reservoir Geophysics", Seismic Data Analysis, 01/01/2001 Publication	<1 %
15	Cox. "Static Corrections—Limitations and Effect on Seismic Data Processes", Static	<1 %

	Corrections for Seismic Reflection Surveys, 01/01/1999 Publication	
16	eprints.upnyk.ac.id Internet Source	<1 %
17	ifg-pub.cen.uni-hamburg.de Internet Source	<1 %
18	tubaf.qucosa.de Internet Source	<1 %
19	Submitted to Curtin University of Technology Student Paper	<1 %
20	arnica.u-strasbg.fr Internet Source	<1 %
21	encyclopedia.pub Internet Source	<1 %
22	hdl.handle.net Internet Source	<1 %
23	pdfcookie.com Internet Source	<1 %
24	www.collectionscanada.ca Internet Source	<1 %
25	Papadimitriou, P.. "Evidence of shear-wave splitting in the eastern Corinthian Gulf (Greece)", Physics of the Earth and Planetary Interiors, 19990706	<1 %

	Publication	
26	dokumen.tips Internet Source	<1 %
27	espace.curtin.edu.au Internet Source	<1 %
28	seg.org Internet Source	<1 %
29	www.ijert.org Internet Source	<1 %
30	www.searchanddiscovery.net Internet Source	<1 %
31	AbdulFattah Al-Dajani, Ilya Tsvankin. "Nonhyperbolic reflection moveout for horizontal transverse isotropy", GEOPHYSICS, 1998 Publication	<1 %
32	Ade Kurniawan, Muhammad Ma'ruf, Respatya Teguh Soewono, Mokhtar, Hari Setiapraja. "A study of fuel consumption on heavy-duty engine fuelled with palm-biodiesel (B30) at various operating condition", AIP Publishing, 2024 Publication	<1 %
33	Jonathan Woodley, Mohammad Mojahedi. "Backward wave propagation in left-handed media with isotropic and anisotropic	<1 %

permittivity tensors", Journal of the Optical Society of America B, 2006

Publication

Exclude quotes	Off	Exclude matches	Off
Exclude bibliography	Off		

The influence of vside-slip velocity

GRADEMARK REPORT

FINAL GRADE

/100

GENERAL COMMENTS

PAGE 1

PAGE 2

PAGE 3

PAGE 4

PAGE 5

PAGE 6

PAGE 7

PAGE 8

PAGE 9

PAGE 10

PAGE 11

PAGE 12

PAGE 13

PAGE 14

PAGE 15

PAGE 16